Geol. Mag. **148** (*1*), *2011, pp. 89–111. © Cambridge University Press 2010*
doi:10.1017/S0016756810000476

Petrogenetic and tectonic inferences from the study of the Mt Cer pluton (West Serbia)

A. KORONEOS*, G. POLI†, V. CVETKOVIĆ‡, G. CHRISTOFIDES*, D. KRSTIĆ§ & Z. PÉCSKAY¶

*Department of Mineralogy, Petrology, Economic Geology, Aristotle University of Thessaloniki, GR-54124 Thessaloniki, Greece
†Department of Earth Sciences, University of Perugia, 06100 Perugia, Italy
‡Faculty of Mining and Geology, University of Belgrade, Đušina 7, 11000 Belgrade, Serbia
§Geospec Consultants Ltd, 4632 151 Street, Edmonton, AB, Canada
¶Institute of Nuclear Research of the Hungarian Academy of Sciences (ATOMKI), Bem ter 18/c, 41001 Debrecen, Hungary

(*Received* 9 July 2009; *accepted* 5 April 2010; *first published online* 15 June 2010)

Abstract – The Mt Cer Pluton, Serbia, is a complex laccolith-like intrusion (~ 60 km^2), situated along the junction between the southern Pannonian Basin and northern Dinarides. It intrudes Palaeozoic metamorphic rocks causing weak to strong thermal effects. Based on modal and chemical compositions, four rock-types can be distinguished: (1) metaluminous I-type quartz monzonite/quartz monzodiorite (QMZD); (2) peraluminous S-type two-mica granite (TMG), which intrudes QMZD; (3) Stražanica granodiorite/quartz monzonite (GDS); and (4) isolated mafic enclaves (ME), found only in QMZD. ^{40}K–^{39}Ar dating and geological constraints indicate that the main quartz monzonite/quartz monzodiorite body of Mt Cer was emplaced not later than 21 Ma, whereas the emplacement ages of the Stražanica granodiorite/quartz monzonite and two-mica granites are estimated at around 18 and 16 Ma, respectively. The Mt Cer pluton is similar to the Mt Bukulja pluton, some 80 km southwestwards. Genesis of QMZD cannot be interpreted by fractional crystallization coupled with mixing or assimilation. It is best explained by a convection–diffusion process between mantle-derived minette/leucominette magmas and GDS-like magmas followed by two end-member magma mixing. The composition of GDS rocks suggests that GDS-like magmas could have formed by melting of lower crustal lithologies similar to amphibolite/metabasalts. The geochemistry of TMG is reproduced by an Assimilation/Fractional Crystallization model with a ratio of rate of assimilation to rate of fractional crystallization of 0.4, using the compositions of the least evolved TMG of the Bukulja pluton and adjacent metamorphic rocks as proxies for the parental magma and contaminant, respectively. The origin and evolution of the Mt Cer and adjacent Mt Bukulja plutons provide new constraints on the Tertiary geodynamics of the northern Dinarides–southern Pannonian region. The quartz monzonite/quartz monzodiorite is interpreted as a result of the Oligocene post-collisional Dinaride orogen-collapse, which included a limited lithosphere delamination, small-scale mantle upwelling, and melting of the lower crust. By contrast, the two-mica granite magmas formed through melting in shallower crustal levels during the extensional collapse in the Pannonian area.

Keywords: South Pannonian Basin, granitoid rocks, leucominettes, convection–diffusion processes, geodynamics.

1. Introduction

The central parts of the Balkan Peninsula in Serbia are characterized by extensive Tertiary calc-alkaline magmatism (e.g. Cvetković *et al.* 2004; Prelević *et al.* 2005; Prelević, Foley & Cvetković, 2007). Along with widespread volcanic rocks, there are numerous granitoid plutons occurring within the composite terranes of the Vardar Zone and Serbo-Macedonian Massif (Fig. 1; e.g. Karamata *et al.* 1992*a*, 1994). They represent part of a regional Tertiary plutonic–volcanic belt stretching from the Periadriatic tonalite line (e.g. von Blanckenburg *et al.* 1992, 1998; von Blanckenburg & Davies, 1995) in the north, through Serbia and further to the SSE in the F.Y.R.O.M. (Former Yugoslav Republic of Macedonia; e.g. Karamata *et al.* 1992*b*), south Bulgaria and northern Greece (e.g. Eleftheriadis *et al.* 1989; Mavroudchiev *et al.* 1993; Christofides *et al.* 1998).

Oligocene plutons are predominant in the area and mainly show I-type characteristics. They originated during post-orogenic dextral transpressional movements associated with wrench tectonics and formation of lacustrine basins along the central axis of the Balkan Peninsula (Fig. 1; Marović *et al.* 2001). The Miocene Mt Cer and Mt Bukulja plutons are located in the southern Pannonian area. These rocks show S-type characteristics and are distinguished from the Oligocene granitoids of the Dinaride suite on the basis of age, petrography, geochemistry and metallogeny (Fig. 1; Steiger, Knežević & Karamata, 1989; Karamata *et al.* 1992*a*).

†Author for correspondence: polig@unipg.it

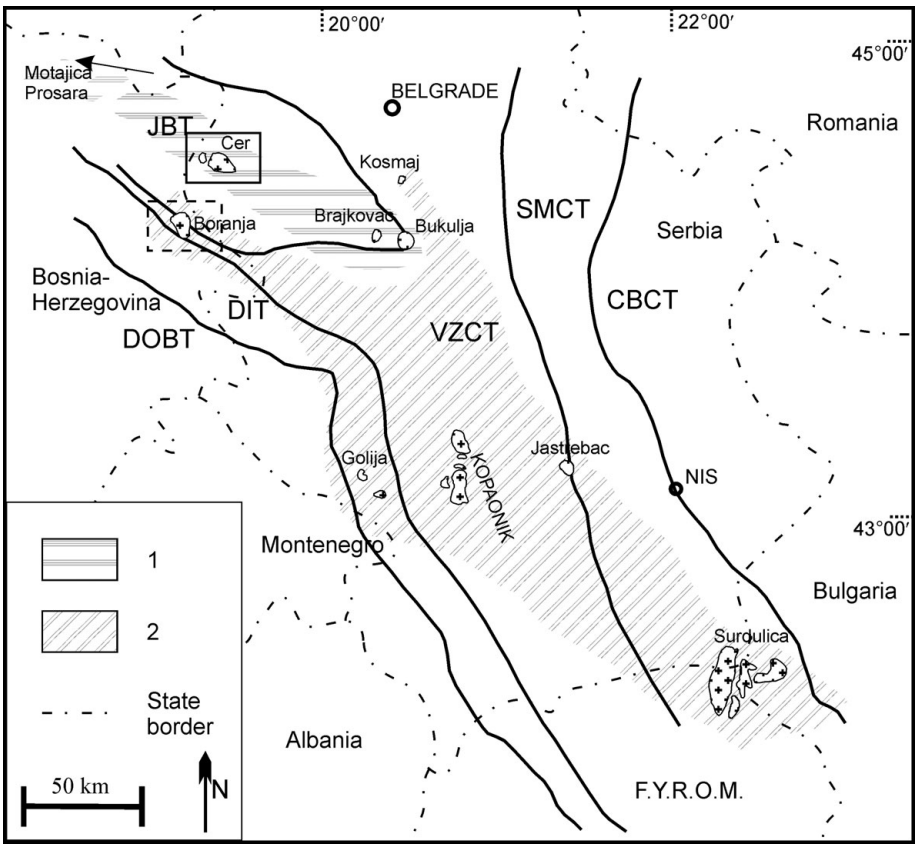

Figure 1. Distribution of Tertiary granitoids of the Balkan Peninsula. Box with solid outline shows the location of the Mt Cer pluton, whereas the dashed line box shows the location of dacites, and minettes/leucominettes from the area of Veliki Majdan. 1 – area of Miocene granitoids cropping out along the southern margin of the Pannonian basin; 2 – area of Oligocene granitoids cropping out in the Dinarides. Geotectonic units/terranes after Karamata *et al.* (1994): DOBT – Dinaride Ophiolite Belt Terrane; DIT – Drina-Ivanjica Terrane; JBT – Jadar Block Terrane; VZCT – Vardar Zone Composite Terrane; SMCT – Serbo-Macedonian Composite Terrane; CBCT – Carpatho-Balkanides Composite Terrane.

The Mt Cer pluton is a composite pluton (Cvetković *et al.* 2002) comprising both I- and S-type granitoid rocks. It is situated at the junction between the northern Dinarides and the southern margin of the Pannonian Basin, and is, hence, a key point for elucidating the geodynamic significance of the Tertiary granitoid magmatism in this part of the Balkan Peninsula.

A precise geodynamic interpretation of the Tertiary granitoids of Serbia and adjacent regions is still a matter of debate. Pamić (1977, 1985/1986) considered all Tertiary granitoids of the central Balkan Peninsula and southern Pannonian domain as related to a magmatic arc setting, suggesting that active subduction processes played an important role in this region during Tertiary times. Pamić, Balen & Herak (2002) argued that these granitoids formed during the Oligocene to Early Miocene post-collision (e.g. Liégeois *et al.* 1998). Cvetković, Knežević & Pécskay (2000), Cvetković *et al.* (2002) and Pécskay *et al.* (2001) gave evidence for post-collisional origin of the Oligocene I-type granites, whereas the Miocene S-type granitoids were interpreted as having resulted after the Pannonian extension.

On the basis of Sr–Nd isotopic data, Steiger, Knežević & Karamata (1989) differentiated Mt Cer rocks into mantle-derived I-type granitoids and upper crustally derived S-type granitoids. This distinction was further supported by Karamata *et al.* (1990, 1992*a*, 1994) and Knežević, Karamata & Cvetković (1994), who reported different ages and metallogenic affinities for the two groups and concluded that I-type and S-type granitoids originated by melting of different crustal materials in response to the uprising of isotherms. Recently, Cvetković *et al.* (2007) argued that the two-mica granites from the Mt Bukulja pluton, situated some 80 km southeast from the Mt Cer pluton, originated during tectonomagmatic events controlled by the early extensional phases during the opening of the Pannonian basin.

In this study we present new geochronological, mineralogical, geochemical and isotope data for Mt Cer granitoids. We compare mineralogical and geochemical characteristics between the Mt Cer and Mt Bukulja granitoid rocks and adjacent lamprophyric rocks of similar age. In particular, the composition of Mt Cer granitoids is compared with the composition of Veliki Majdan minettes/leucominettes and dacites situated a few tens of kilometres to the southwest (Prelević *et al.* 2004). We develop the idea of Cvetković *et al.* (2007), who suggested that the Mt Bukulja and Mt Cer plutons are petrogenetically linked, and that lamprophyric magmas have probably played an important role in the

https://doi.org/10.1017/S0016756810000476 Published online by Cambridge University Press

genesis of the Mt Bukulja pluton. The present work aims to clarify the origin and evolution of the Mt Cer pluton and to elucidate timing and petrogenesis of two different magmatic episodes interpreted as the result of slight changes in geodynamic conditions.

2. Geology and petrography of the Mt Cer pluton

The Mt Cer pluton is an E–W-elongated laccolith-like intrusion covering an area of about 60 km^2 (Figs 1, 2). The country rocks are, in fact, dipping periclinally from the pluton and the angles are less steep in the eastern and western parts. The pluton intrudes metamorphic rocks of Jadar Block Terrane (Karamata *et al.* 1994), made by a Middle Devonian to Early Permian series composed of weakly metamorphosed sedimentary protoliths now mostly represented by phyllites and sericite–chlorite and chlorite schists (Filipović, Sikošek & Jovanović, 1993) metamorphosed under greenschist-facies conditions. These metamorphic rocks surround the whole pluton except in the south, where the pluton is cut by the E–W-oriented Lešnica normal fault (Fig. 2). Geophysical data (Labaš, 1975) revealed a negative gravimetric anomaly with a maximum around 5 km to the south of the Lešnica structure, implying that the pluton continues southwards. This part is today covered by 600–800 m thick Miocene breccias containing granite boulders. Thus, only the northern edge of the exposed intrusive body corresponds to the real margin of the pluton. The Stražanica intrusion crops out in the northwest as an N–S-elongated small body (~ 7 km^2) separated from the main pluton by a narrow belt of contact-metamorphosed rocks (Fig. 2). It is worth noting that thermal metamorphic effects are weaker around the main body (from rocks unaffected by contact metamorphic to tourmaline hornfels) and stronger around the Stražanica intrusion (andalusite-, biotite- and (rarely) garnet-bearing spotted hornfels: Knežević, 1962). Such different metamorphic assemblages can be explained by contact metamorphism occurring at higher and lower pressures, around the main body and the Stražanica intrusion, respectively. Petrofabric investigations reveal the presence of a foliated magmatic fabric in the northern margin of the pluton, represented by northerly dipping mica flakes and elongated crystals of plagioclase and hornblende. Other Mt Cer granitoid lithologies do not show detectable microfabric anisotropy.

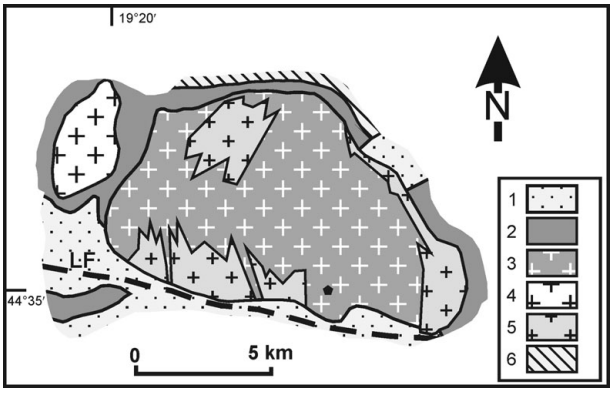

Figure 2. Simplified geological sketch map of the Mt Cer composite pluton. 1 – Neogene and Quaternary sediments; 2 – contact metamorphic rocks; 3 – quartz monzonites to quartz monzodiorites (QMZD); 4 – granodiorites to quartz monzonites from Stražanica (GDS); 5 – areas of occurrence of two-mica granites (TMG); 6 – Palaeozoic schist. Black pentagon – area of occurrence of large enclave; LF – Lešnica fault (mostly covered).

The Mt Cer granitoids are classified following the classification scheme of Streckeisen & Le Maitre (1979) (Fig. A1; online Appendix at http://journals.cambridge.org/geo), and on the basis of petrography. Three main groups of rocks can be recognized: quartz monzonites to quartz monzodiorites (QMZD), two-mica granites (TMG), and Stražanica granodiorites to quartz monzonites (GDS). The spatial distribution of the various rock types is shown in Figure 2.

Quartz monzodiorite rocks compose the central parts of Mt Cer constituting around 60 vol. % of the whole pluton. They crop out within deep creeks as well as on some hills. Two-mica granites are found in the eastern, northwestern and southwestern peripheral parts of the Mt Cer pluton (Fig. 2). They occur as metre-thick veins, dykes, or larger irregular bodies and always show sharp contacts towards QMZD. Stražanica granodiorites to quartz monzonites constitute a quite homogeneous body situated at the northwesternmost side of Mt Cer.

Quartz monzodiorite rocks are grey to dark grey in colour, massive but with some magmatic foliation in the northern parts. The texture is allotriomorphic granular, but porphyritic varieties with large grains of K–feldspar also occur. Selected chemical microprobe analyses of feldspars, biotite, muscovite and amphibole are reported in Table A1 (online Appendix at http://journals.cambridge.org/geo). Xenomorphic and undulose quartz (~ 27 vol. %), K–feldspar (~ 26 vol. %; $Or_{87.3–90.0}$), plagioclase (~ 30 vol. %; $An_{31.3–37.3}$/cores to $An_{29.9–35.8}$/rims), biotite (8–18 vol. %), and hornblende (0–8 vol. %) are the main constituents of QMZD, whereas titanite, allanite, magmatic epidote, zircon, apatite, rutile, magnetite and ilmenite are present as accessory minerals.

Two-mica granites are fine- to medium-grained, white-grey in colour with hypidiomorphic granular texture and massive structure. They mainly consist of quartz, (29–41 vol. %), K-feldspar (27–38 vol. %; $Or_{86.5–90.1}$), plagioclase (14–32 vol. %; $An_{8.7–13.4}$/cores to $An_{7.8}$/rims), muscovite (5–15 vol. %) and biotite (usually <5 vol. %), as well as accessory garnet, tourmaline, apatite, rutile and zircon.

Stražanica granodiorite to quartz monzonite rocks are light-grey in colour and display a uniform hypidiomorphic medium-grained texture. They are composed of quartz (~ 25 vol. %), plagioclase (~ 47 vol. %; $An_{26.4}$/cores to $An_{21.1}$/rims), K–feldspar (~ 15 vol. %; $Or_{91.6}$), and biotite (~ 10 vol. %), while zircon, allanite, apatite, muscovite, epidote and titanite are accessory phases.

https://doi.org/10.1017/S0016756810000476 Published online by Cambridge University Press

Mafic enclaves (ME) are found in QMZD exclusively. They crop out only in the marginal parts of QMZD as scarce dark-green elongated schlieren and lensoidal to rounded enclaves. They are around 5 × 10 cm in size, rarely smaller, and show a hypidiomorphic granular texture. They have amphibole (up to 73 vol. %), plagioclase (~ 16 vol. %; $An_{31.3}$/cores to $An_{33.3}$/rims) and biotite (~ 8 vol. %) as main constituents, and K–feldspar (Or_{88}), titanite, apatite, allanite and epidote as accessory minerals. On the southern slopes of Mt Cer, a large (1 × 1.5 m) mafic enclave was found in QMZD (Knežević, Karamata & Cvetković, 1994). This enclave is substantially richer in biotite (~ 45 vol. %) and K–feldspar (~ 28 vol. %) and poorer in plagioclase (~ 15 vol. %) and amphibole (~ 10 vol. %), in comparison to the smaller mafic enclaves. Knežević, Karamata & Cvetković (1994) argued for a lamprophyric character for this mafic enclave because they found higher MgO contents in biotite and hornblende from the enclave than in biotite and hornblende from the host rock (QMZD). Unfortunately, this lithology is no longer available for sampling due to the extensive cover, ruling out more detailed study of this type of enclaves.

The dominant ferromagnesian phase in all the rock types is biotite, except in the enclaves where hornblende prevails. Determination of the biotite composition was made for the main groups of Mt Cer rocks. In an Al_{tot} v. Fe no. plot (Fig. 3a) the compositions of most QMZD biotites plot in the minette/leucominette field, as do the compositions of biotites from enclaves, which display, however, lower Fe no. values. By comparison, biotites from hornblende–biotite granites (H-BG) of Mt Bukulja (Cvetković *et al.* 2007) have the same Al_{tot} range, but higher Fe no. than biotites from QMZD. Biotites from TMG are compositionally similar to those from two-mica granites from Mt Bukulja and have high Fe no., as expected for such evolved rock compositions.

Mafic enclave and quartz monzonite/quartz monzodiorite rocks were selected for plagioclase–hornblende thermobarometry. All selected samples have a mineral assemblage of plagioclase, hornblende, K-feldspar, biotite, titanite, magnetite and quartz, which is an important prerequisite for applying aluminium-in-hornblende barometry (e.g. Hammarstrom & Zen, 1986; Schmidt, 1992; Anderson & Smith, 1995; Stein & Dietl, 2001). Because the influence of temperature (and oxygen fugacity) on pressure calculations has to be considered, we have chosen the calibration of Anderson & Smith (1995) to calculate crystallization pressures. Equilibration temperatures for hornblende–plagioclase assemblages were calculated on the basis of iterations started from pressures calculated using Anderson & Smith (1995) and using various thermometers. Preferred values according to Anderson (1996) have been accepted (see also Anderson *et al.* 2008; Holland & Blundy, 1994). Accordingly, temperature and pressure values were calculated

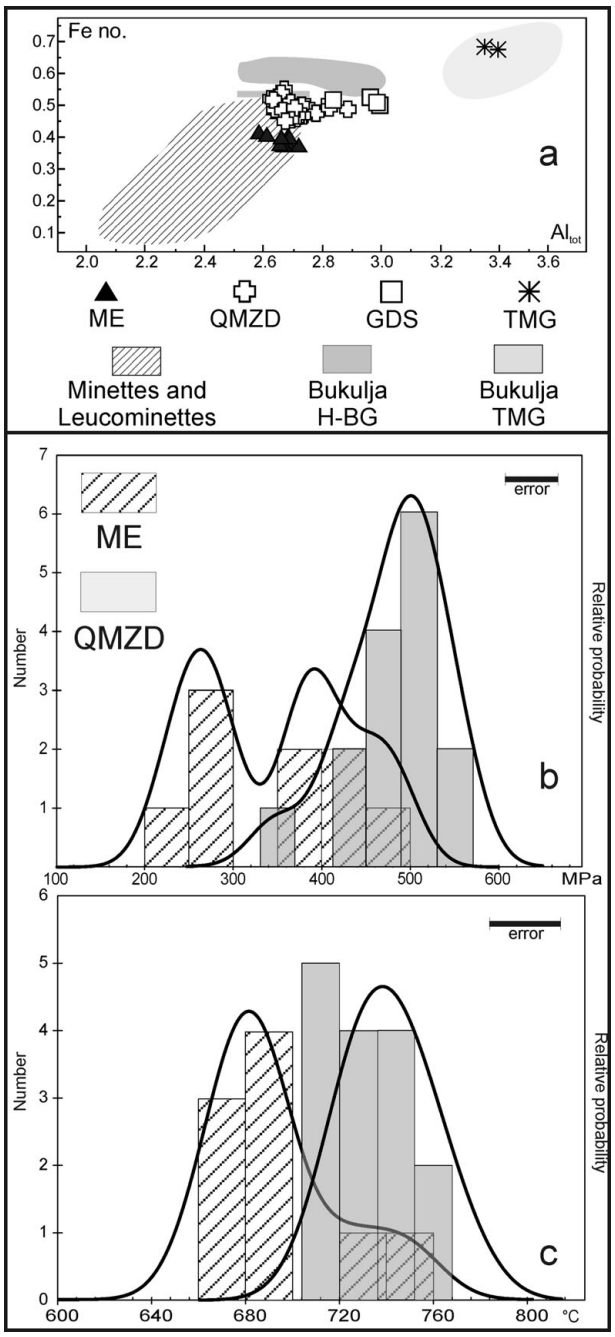

Figure 3. Al_{tot} v. Fe/(Fe+Mg) (Fe no.; cation basis) diagram showing the chemical compositions of biotite of the Mt Cer granitoid (a). The compositions of biotites of H-BG (hornblende–biotite granite) and TMG (two-mica granite) rocks from Bukulja pluton (Cvetković *et al.* 2007) and of minettes/leucominettes from Veliki Majdan (Prelević *et al.* 2004) are also displayed. (b) and (c) show probability density distribution diagrams for analysed amphibole for pressure (MPa) and temperature (°C), respectively. The number of analyses is 15 and 9 for QMZD and ME, respectively.

using Microsoft Excel spreadsheet 'Plagioclase–Hornblende Thermobarometry' (Anderson *et al.* 2008: http://www.minsocam.org/MSA/RIM/ RiM69_Ch04_hbld_plag_thermo-jla.xls).

Histograms of pressure (Fig. 3b) and temperature (Fig. 3c) estimates for amphibole rims are reported

https://doi.org/10.1017/S0016756810000476 Published online by Cambridge University Press

Table 1. New and published ^{40}K–^{39}Ar ages of Mt Cer granitoid rocks

Rock type	Sample	Dated fraction	K (%)	^{40}Ar rad (%)	^{40}Ar rad ccSTP/g	Age (Ma)	Reference
Enclaves (ME)							
	C-5	Biotite	5.63	39.0	4.122×10^{-6}	18.74 ± 0.88	Knežević, Karamata & Cvetković, 1994
		Feldspars (Kf+Plg)	6.84	75.0	4.683×10^{-6}	17.54 ± 0.67	
		Amphibole	0.85	23.3	8.574×10^{-7}	25.90 ± 1.7	
Quartz monzonites to quartz monzodiorites (QMZD)							
	C-3	Biotite	4.83	77.1	3.247×10^{-6}	17.22 ± 0.66	This work
		Feldspars	2.07	87.5	1.336×10^{-6}	16.48 ± 0.62	
		Hornblende	0.86	20.1	7.127×10^{-7}	21.11 ± 1.55	
Granodiorites to quartz monzonites from Stražanica (GDS)							
	C-4	Biotite	6.63	81.0	4.445×10^{-6}	17.17 ± 0.65	Knežević, Cvetković & Resimić, 1997
		Feldspars	0.85	50.8	6.392×10^{-7}	19.10 ± 0.80	
Two-mica granites (TMG)							
	C-1	Muscovite	8.55	59.9	5.333×10^{-6}	15.96 ± 0.64	This work
		Biotite	5.81	53.6	3.604×10^{-6}	15.98 ± 0.65	
		Feldspars	4.88	72.2	2.872×10^{-6}	15.10 ± 0.58	
	C-2	Muscovite	8.11	66.3	5.214×10^{-6}	16.48 ± 0.65	
		Feldspars	3.35	79.6	1.988×10^{-6}	15.20 ± 0.60	

as probability density plots. Although the errors for both geobarometer and geothermometer are high, owing to errors connected with regression of data, chosen temperature values and analytical imprecision, the values of around 60 MPa and 30 °C can be considered conservative for pressure and temperature, respectively (e.g. Zhang, Zhao & Song, 2006). On the other hand, our goal was to discuss differences in crystallization pressures between QMZD and ME, rather than estimating the absolute values. The ranges of crystallizing pressures and temperatures for QMZD rocks are 350–550 MPa and 700–770 °C, respectively. The maximal crystallizing pressure for QMZD rocks is about 500 MPa with a minimum at lower pressures at about 350 MPa. The maximum temperature is estimated at about 730 °C. Estimated crystallizing pressures for ME rocks have two peaks at 400 MPa and 250 MPa, whereas the maximum temperature is 680 °C with a lower peak at about 740 °C. Although there is a clear overlap of data, QMZD and ME rocks show different crystallizing pressures and temperatures. Relatively higher pressures obtained for QMZD are in accordance with the presence of primary magmatic epidote in some QMZD samples (e.g. Zen & Hammarstrom, 1984; Vyhnal, McSween & Speer, 1991).

2.a. Age

New and available radiometric data (Table 1), along with geological and petrological evidence, provide some constraints for the age interpretation. ^{40}K–^{39}Ar data on hornblende reveal ages of *c.* 21 Ma for QMZD, whereas biotite and feldspars (Kf + Plg) from the same rock give younger ages (17–16 Ma). The GDS biotite and feldspar fractions (Kf + Plg) yielded ages of *c.* 17 Ma and 19 Ma, respectively. The pressure estimates for QMZD rocks (~ 400–600 MPa) imply that these rocks have started to crystallize rather deep in the crust, in accordance with a weak contact–metamorphic aureole. Consequently, the ^{40}K–^{39}Ar hornblende age of QMZD (*c.* 21 Ma) can be regarded as a minimum emplacement age, whereas the ^{40}K–^{39}Ar determinations on biotite can be regarded as minimum cooling ages. On the other hand, the possibility that the intrusion of TMG could have induced thermal rejuvenation effects on micas and feldspars of older ME and QMZD seems unlikely, because TMG intrude the QMZD body only locally, and therefore the thermal effect must have been more localized. Much stronger contact-metamorphic effects around GDS suggest that their crystallization and emplacement must have occurred in shallower levels. The ^{40}K–^{39}Ar estimate on GDS biotite can be regarded as a minimum cooling age, and the similarity with the age obtained on QMZD biotite could indicate that GDS and QMZD crystallized roughly contemporaneously. Feldspars (Kf + Plg) and muscovite from TMG rocks gave the youngest ages and the lowest age range of 15–16 Ma; this is in accordance with the mode of their occurrence. Two-mica granites sharply cut the QMZD rocks, hence they must have been emplaced during the final stage of the evolution of the Mt Cer pluton. A mafic enclave sample exhibits the largest age range, from around 26 Ma obtained on hornblende to around 18 Ma and 17 Ma obtained on biotite and feldspars (Kf + Plg), respectively. The values of 26 and 18 Ma cannot be considered as minimum initial crystallization and cooling ages, respectively, because 8 Ma is too large a time span from the onset of crystallization to its termination for such a small (decimetric) magmatic body. Consequently, we consider the estimated value of 26 Ma as having resulted from Ar retention, which often happens in K/Ar dating of hornblende (e.g. McDougall & Harrison, 1999). On the other hand, the ^{40}K–^{39}Ar biotite age of 18 Ma can be regarded as a minimum cooling age. It is noteworthy that such an age is similar to the ^{40}K–^{39}Ar biotite age obtained for QMZD.

https://doi.org/10.1017/S0016756810000476 Published online by Cambridge University Press

3. Geochemical characterization of the Mt Cer granitoid rocks

On the basis of their spatial distribution, mineralogy, texture and extent of alteration, nineteen samples were selected for major and trace element analyses (Table 2). Nine samples were analysed also for REE (Rare Earth Elements; Table 3), and seven samples for Sr and Nd isotopes (Table 4). In addition, major element and Sr isotope data for six samples were taken from the literature (Karamata *et al.* 1990; Knežević, Cvetković & Resimić, 1997). Analytical techniques are reported in the Appendix A1 available online at http://journals.cambridge.org/geo.

This study reveals complex spatial–chemical relationships between the above-described types of granitoid rocks. Quartz monzonite/quartz monzodiorite rocks predominantly show a high-K calc-alkaline affinity, whereas TMG samples plot in the high-K calc-alkaline–shoshonitic fields according to Peccerillo & Taylor (1976) (Fig. A2; online Appendix at http://journals.cambridge.org/geo). Mafic enclaves are variable but shoshonitic in character, whereas GDS samples are mainly medium-K calc-alkaline. Quartz monzonite/quartz monzodiorite rocks and GDS are metaluminous, whereas TMG are peraluminous with ASI up to 1.35. Petrographic and geochemical characteristics indicate that QMZD and GDS are I-type rocks, whereas TMG are S-type rocks.

Contents of some major oxides and trace elements (TiO_2, CaO, P_2O_5, V, Co, Cr, Zr, Ba; Fig. 4a) follow a single trend from minettes/leucominettes of the Veliki Majdan area (Prelević *et al.* 2004) to two-mica granites from both the Mt Cer and Mt Bukulja plutons. Al_2O_3, Na_2O, Fe_2O_{3tot} and Y contents (Fig. 4b) are uniform in intermediate-acid rocks, but increase noticeably from minettes/leucominettes to dacites. K_2O, Rb, Th and Nb concentrations (Fig. 4c) follow a trend from minettes/leucominettes to two-mica granites, although the latter samples are very scattered. Quartz monzonite/quartz monzodiorite and GDS samples plot at the lower end of the trend formed by dacite of the Veliki Majdan area (Prelević *et al.* 2004) and Mt Bukulja hornblende–biotite granites (H-BG), whereas TMG samples from Mt Cer plot at the upper end of the TMG Mt Bukulja group. The behaviour of Sr contents (Fig. 4d) is peculiar: minettes/leucominettes, dacites, all the Mt Bukulja rocks, and TMG rocks from Mt Cer follow a single trend, whereas QMZD and GDS samples show distinctively higher Sr contents. Regarding the ME group, the three ME samples, as already mentioned, have heterogeneous compositions. The sample poorest in SiO_2 does not fit to any of the groups reported in Figure 4, whereas the other two samples plot within the dacite group for many elements, except for K_2O, Rb, Th, Nb and Sr. In addition, the two ME samples with similar SiO_2 contents show remarkable differences in K_2O, Rb, Th and Nb contents.

Rare earth element patterns are fractionated and total REE contents decrease from ME to TMG (Fig. 5a). REE concentrations decrease also from minette/leucominette to TMG (Fig. 5b–d), and mimic the trend followed by K_2O (Fig. 4c). The negative Eu-anomaly slightly decreases from minette/leucominette to hornblende–biotite granite, whereas it displays high values in both Mt Bukulja and Mt Cer two-mica granite (Fig. 5e). Values of $(La/Yb)_n$ are very scattered for all groups of samples, with minette/leucominette plotting into two quite distinct areas (Fig. 5f).

Quartz monzonite/quartz monzodiorite and dacite samples from the Veliki Majdan area show similar primitive mantle-normalized spider diagram patterns, except for Sr and Nb (Fig. 6a). On the other hand, two-mica granites from Mt Cer display similar patterns to those shown by TMG from Mt Bukulja (Fig. 6b), whereas GDS rocks show no geochemical similarities either with TMG or with QMZD rocks (Fig. 6b).

Sr and Nd isotope compositions are shown in Figure 7. Generally, the initial $^{87}Sr/^{86}Sr$ and $^{143}Nd/^{144}Nd$ ratios decrease and increase with evolution, respectively. Quartz monzonite/quartz monzodiorite rocks have similar isotopic compositions to dacites of the Veliki Majdan area, whereas TMG rocks from Mt Cer exhibit the highest $^{87}Sr/^{86}Sr_i$ and the lowest $^{143}Nd/^{144}Nd_i$ values of the entire suite. It is noteworthy that two-mica granites from Mt Cer and Mt Bukulja are different in terms of Sr and Nd isotopes.

4. Discussion of source and evolution processes

Any petrogenetic model intended to explain the genesis and differentiation of the granitoid facies of the Mt Cer pluton must take into account their field, petrographic and geochemical characteristics, namely: (1) lack of clear evidence of magma interaction both from a petrographic and geochemical point of view; (2) compositional similarity between QMZD and dacites of the Veliki Majdan area, the latter being genetically related to minettes/leucominettes (Prelević *et al.* 2004); (3) major and trace element compositional similarity between Mt Cer and Mt Bukulja TMG rocks, while having different Sr–Nd isotope ratios; (4) geochemical and isotope dissimilarity between GDS and any other above-mentioned rock group.

In the following discussion, we try to unravel source and evolution processes of each granitoid facies, also aiming to understanding their mutual genetic relationships.

4.a. QMZD

An important issue in deciphering the origin and evolution of the main body of the Mt Cer pluton is the petrogenetic significance of the ME group. Following the classification of Didier & Barbarin (1991), mafic enclaves could be either ‘mafic microgranular enclaves’

https://doi.org/10.1017/S0016756810000476 Published online by Cambridge University Press

Table 2. XRF chemical analyses of major (wt%) and trace element (ppm) contents of selected samples from the Mt Cer pluton

Rock type	Enclaves (ME)			Quartz monzonites to quartz monzodiorites (QMZD)										Granodiorites to quartz monzonites (GDS)					Two mica granites (TMG)						
Sample no.	113a	112	100x	C88–2*	108	100	109	113	102	101	103	111	C89–3†	115	STR100	C89–6§	114	C89–5§	107	110	105	104	C89–4†	C88–1*	106
SiO_2	52.79	59.37	59.44	57.80	60.73	60.87	61.95	62.70	63.13	63.89	64.05	64.37	65.86	67.54	67.82	68.58	69.89	70.47	69.64	71.31	71.55	71.8	72.3	72.33	72.67
TiO_2	0.96	0.87	0.80	0.67	0.76	0.68	0.61	0.54	0.59	0.52	0.52	0.55	0.50	0.32	0.28	0.34	0.29	0.08	0.24	0.07	0.14	0.13	0.08	0.13	0.17
Al_2O_3	15.87	13.96	14.13	16.83	16.55	16.44	16.20	16.14	16.24	15.72	16.37	16.22	17.18	16.40	16.22	16.47	15.34	15.38	16.51	15.39	15.21	14.81	16.10	15.69	14.31
Fe_2O_3	4.78	3.38	6.00	3.41	3.30	2.45	2.89	3.90	3.83	3.01	1.92	3.20	0.94	2.35	1.72	1.11	1.49	2.25	1.38	1.01	1.34	1.07	0.80	1.31	1.29
FeO	4.40	1.32	1.16	5.70	2.48	2.74	2.45	1.04	1.18	1.73	2.47	1.05	2.64	0.34	0.68	1.67	0.88	1.49	0.11	0.22	0.11	0.42	0.78	0.47	0.18
MnO	0.20	0.10	0.17	0.16	0.12	0.12	0.12	0.12	0.12	0.12	0.11	0.10	0.10	0.08	0.08	1.27	0.07	0.03	0.06	0.07	0.06	0.07	0	0.02	0.06
MgO	4.40	4.75	4.41	2.95	2.27	2.15	2.12	1.92	1.86	1.99	1.62	1.52	2.30	0.73	0.64	0.06	0.64	0.99	0.20	0.13	0.22	0.23	0.95	0.56	0.20
CaO	6.91	4.70	5.61	6.85	5.29	5.59	4.77	4.56	4.76	4.11	4.10	4.61	3.74	3.17	3.37	2.98	2.92	2.90	1.30	1.07	1.31	1.29	1.25	1.28	1.34
Na_2O	3.09	1.92	2.90	2.32	4.13	3.91	3.78	3.76	3.82	3.55	4.11	4.31	2.54	5.26	5.56	3.66	5.80	4.20	3.35	4.27	3.84	3.34	2.77	3.18	3.26
K_2O	4.50	8.29	3.65	2.00	2.99	3.42	3.56	4.31	3.45	4.26	3.59	3.10	3.78	3.06	2.92	2.57	2.06	2.03	6.17	5.58	5.13	5.62	4.70	5.40	5.68
P_2O_5	0.80	0.54	0.74	0.02	0.33	0.33	0.33	0.32	0.29	0.32	0.27	0.25	0.14	0.16	0.15	0.10	0.14	0.10	0.20	0.13	0.20	0.23	0.02	0.05	0.19
LOI	1.31	0.79	1.00	0.93	1.05	1.30	1.21	0.69	0.74	0.76	0.88	0.71	0.20	0.59	0.55	0.72	0.48	0.33	0.83	0.75	0.89	0.98	0.70	0.28	0.64
V	167	86	94	–	89	86	82	78	77	69	56	61	–	8	23	–	17	–	6	6	6	6	–	–	6
Cr	51	237	269	–	49	53	40	46	35	43	30	37	–	18	14	–	14	–	3	10	10	4	–	–	9
Co	22	17	18	–	9	5	6	6	6	8	6	10	–	0	5	–	4	–	7	2	1	2	–	–	2
Ni	42	102	102	–	16	21	12	16	18	16	16	17	–	8	6	–	7	–	14	14	15	13	–	–	11
Ga	24	14	18	–	24	20	24	18	21	17	21	19	–	18	19	–	18	–	29	27	20	23	–	–	20
Cu	12	38	15	–	26	20	16	16	19	15	12	18	–	12	8	–	10	–	5	14	6	8	–	–	6
Zn	117	80	112	–	85	79	97	66	71	74	132	59	–	41	36	–	37	–	44	72	42	47	–	–	46
Rb	164	411	181	125	143	137	171	142	172	194	237	189	132.5	74	78	73	61	61	291	330	265	268	312	241	271
Sr	728	862	678	852	792	782	836	845	817	810	728	777	799	735	694	691	580	588	113	91	97	102	77	84	119
Y	48	13	30	–	18	16	17	15	18	16	13	16	–	6	6	–	8	–	9	20	13	12	–	–	10
Zr	247	344	266	–	183	179	203	166	183	159	167	171	–	122	114	–	113	–	76	34	51	52	–	–	81
Nb	20	14	14	–	14	10	13	11	10	11	11	12	–	5	5	–	6	–	11	17	10	10	–	–	7
Ba	1478	1462	1047	–	595	867	1051	1318	1155	965	837	1043	–	827	810	–	433	–	320	147	229	236	–	–	351
La	39	35	27	–	25	27	47	25	33	24	33	29	–	28	23	–	27	–	19	21	18	14	–	–	30
Ce	81	115	37	–	45	42	71	51	35	53	49	48	–	24	6	–	21	–	12	8	5	21	–	–	14
Pb	45	57	35	–	37	41	42	41	44	46	39	44	–	47	44	–	32	–	50	51	54	58	–	–	50
Th	22	23	14	–	16	18	29	18	22	22	23	26	–	15	8	–	6	–	15	9	9	10	–	–	13
Sr/Y	15.2	66.3	22.6	–	44.0	48.9	49.2	56.3	45.4	50.6	56.0	48.6	–	122.5	115.7	–	72.5	–	12.6	4.6	7.5	8.5	–	–	11.9
ASI	0.74	0.70	0.78	0.88	0.86	0.83	0.88	0.86	0.89	0.90	0.92	0.88	0.94	1.08	0.98	1.15	1.04	1.09	1.35	1.17	1.04	1.13	1.14	1.05	0.97

*From Karamata *et al.* 1990. †From Knežević, unpub. data. §From Knežević, Cvetković & Resimić, 1997. ASI (aluminum-saturation index) = molecular Al/(Ca+1.67*P+Na+K).

Table 3. Rare earth element and trace element contents for representative Mt Cer granitoids, analysed by ICP-MS

Rock type	Sample	La	Ce	Pr	Nd	Sm	Eu	Gd	Tb	Dy	Ho	Er	Tm	Yb	Lu	Pb	U	Th	(La/Yb)n	Eu*
Enclaves (ME)																				
	113a	57	113	14	56	13	2.8	12	1.5	8.7	1.4	3.7	0.58	3.5	0.54	45	4.0	25	0.66	9.7
	100x	29	61	8.3	35	8.0	1.8	6.6	0.87	5.2	0.86	2.2	0.32	1.7	0.33	29	2.1	8.8	0.74	10.2
Quartz monzonites to quartz monzodiorites (QMZD)																				
	113	38	71	8.2	30	6.1	1.5	6.5	0.63	3.8	0.66	1.5	0.22	1.4	0.21	41	6.2	16	0.72	16.6
	101	41	75	8.6	32	6.2	1.5	5.9	0.55	3.5	0.53	1.4	0.25	1.3	0.27	58	3.9	18	0.74	18.6
	103	33	61	7.4	26	5.4	1.3	5.0	0.47	2.9	0.51	1.1	0.19	1.2	0.22	34	3.0	15	0.76	17.3
Granodiorites to quartz monzonites from Stražanica (GDS)																				
	115	22	42	4.8	18	3.3	0.87	3.2	0.31	1.8	0.21	0.78	0.09	0.66	0.10	41	2.0	7.8	0.81	20.4
	STR100	18	34	4.0	14	2.9	0.90	2.9	0.28	1.9	0.32	0.78	0.10	0.77	0.12	44	7.3	6.6	0.95	14.1
Two-mica granites (TMG)																				
	107	19	40	4.7	17	4.0	0.54	2.7	0.32	1.8	0.23	0.52	0.07	0.36	0.06	5	2.1	10	0.48	31.9
	105	11	24	3.1	11	2.9	0.56	2.3	0.39	2.3	0.26	0.57	0.09	0.54	0.05	57	5.9	5.8	0.65	12.8

Eu* = Eu anomaly, calculated by dividing the chondrite-normalized Eu concentration of a rock by the half-sum of the normalized concentrations of Sm and Gd.

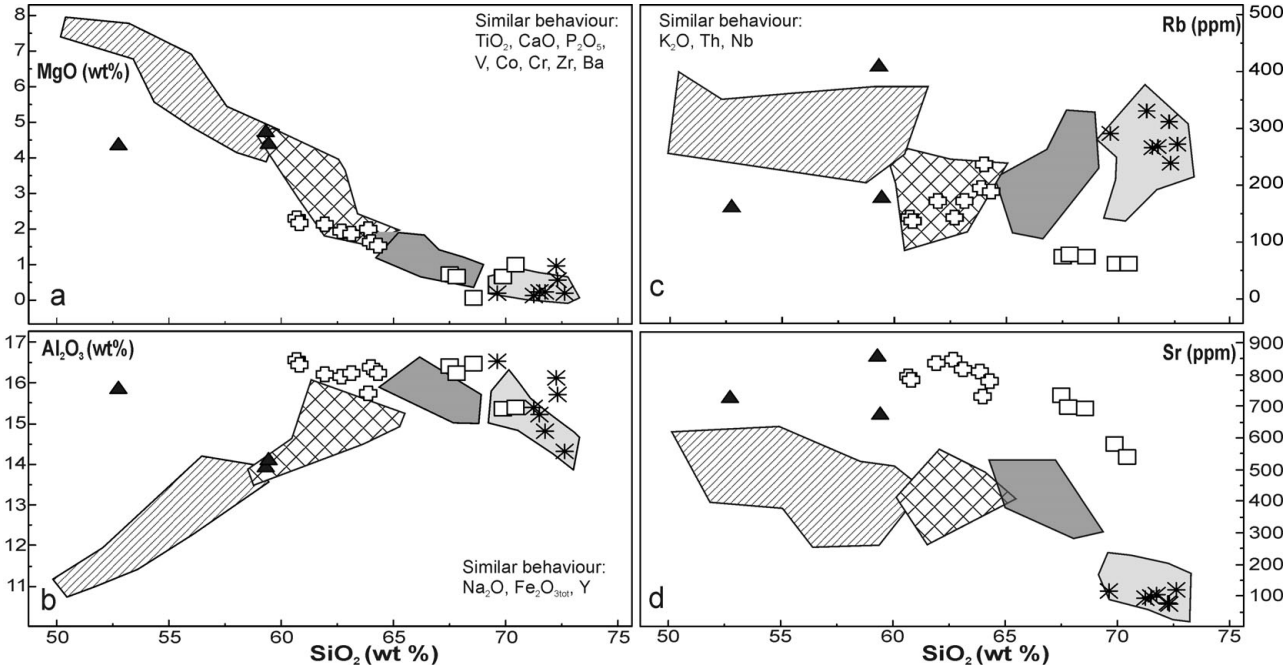

Figure 4. Major and trace element variation diagrams for the Mt Cer plutonic rocks. The whole rock composition of H-BG and TMG rocks from the Mt Bukulja pluton (Cvetković *et al.* 2007), as well as dacites (square hatched field) and minettes/leucominettes from Veliki Majdan (Prelević *et al.* 2004) are also shown. Other symbols as in Figure 3.

(hereafter MME), implying that they derive from interaction processes between different magma batches (e.g. Poli, Tommasini & Halliday, 1996; Janousek *et al.* 2004), or cognate enclaves, suggesting that they represent accumulations of fractionated phases (e.g. Nitoi *et al.* 2002; Donaire *et al.* 2005).

Structures found in the field are important for deciphering the true genesis of enclaves. The Mt Cer ME are found in the peripheral parts of the QMZD body and they are all decimetric in size with only a few smaller enclaves. These are uncommon features for MME, because the MME are commonly found throughout the plutons, and they have different dimensions (e.g. Barbarin & Didier, 1991). The ME samples have lobate and rounded shapes exhibiting rare chilled margins. These features are common both in MME (Blake & Fink, 2000) and cognate enclaves (Nitoi *et al.* 2002), and it is not uncommon to find them occurring contemporaneously in the same MME enclave. These findings cannot give unequivocal indications as to the real nature of the ME rocks. A very common MME feature at the macro-scale is the occurrence of host-derived crystals (usually plagioclase, K-feldspar, biotite), either within the enclaves or even cross-cutting the contacts between the enclaves and host (e.g. Collins *et al.* 2000; Barbarin, 2005). These features are considered as proofs of mass transfer between the interacting magmas and as indications that the enclaves were in a liquid state upon their incorporation into the more felsic magma (e.g. Vernon, 1984; Castro, Mereno-Ventas & de la Rosa, 1991; Perugini *et al.* 2003). However, this feature is lacking in the ME rocks both in the field and on a thin-section scale.

Apart from the large enclave found in the southern part of the pluton, the mineralogical assemblage

https://doi.org/10.1017/S0016756810000476 Published online by Cambridge University Press

Table 4. Sr and Nd isotopic compositions of representative Mt Cer granitoids

Rock type	Sample	Rb	Sr	$^{87}Rb/^{86}Sr$	2σ	$(^{87}Sr/^{86}Sr)_m$	2σ	$(^{87}Sr/^{86}Sr)_{20Ma}$	2σ	Sm	Nd	$^{147}Sm/^{144}Nd$	2σ	$(^{143}Nd/^{144}Nd)_m$	2σ	$(^{143}Nd/^{144}Nd)_{20Ma}$	2σ
Enclaves (ME)																	
	113a	117.37	672.84	0.5	4	0.708416	19	0.708273	22	4.99	22.09	0.64	5	0.512385	8	0.512301	10
Quartz monzonites to quartz monzodiorites (QMDZ)																	
	C88–2	125	852.2	0.42	3	0.708207	33	0.708086	34	5.7	36.2	0.45	4	0.512366	–	0.512308	n.d.
	100	148.98	612.9	0.7	5	0.708525	19	0.708325	25	7.44	31.39	0.67	5	0.512362	9	0.512274	11
	113	144.67	754.62	0.55	4	0.708284	18	0.708126	22	6.15	33.17	0.53	4	0.512435	12	0.512366	13
	101	166.02	742.55	0.64	5	0.708408	17	0.708224	22	6.08	35.61	0.48	4	0.512379	7	0.512316	9
	103	210.09	670.31	0.91	7	0.708534	15	0.708276	25	4.85	25.84	0.53	4	0.512332	34	0.512262	34
	C89–3	132.5	799.8	0.48	4	0.708374	22	0.708238	25	5.677	52.59	0.31	2	0.512343	n.d.	0.512303	n.d.
Granodiorites to quartz monzonites from Stražanica (GDS)																	
	115	62.52	654.72	0.27	2	0.707109	17	0.707031	18	2.72	14.06	0.55	4	0.512426	12	0.512354	13
	C89–6	73	691	0.328	2	0.707049	29	0.706961	30	2.883	14	0.58	5	0.512406	n.d.	0.51233	n.d.
	C89–5	61	588	0.309	2	0.706637	42	0.706544	43	2.619	13	0.57	5	0.512403	n.d.	0.512328	n.d.
Two-mica granites (TMG)																	
	C88–1	241	84	8.3	7	0.72131	34	0.71855	218	9.8	42.5	0.65	5	0.512132	n.d.	0.512046	n.d.
	105	215.01	91.2	6.82	7	0.722183	17	0.720243	156	3.23	10.83	0.85	7	0.512137	9	0.512026	13
	C89–4	312	76.72	11.7	9	0.719714	25	0.716368	269	5.59	29.49	0.54	4	0.512121	n.d.	0.512051	n.d.

References for published samples are given in Table 2. n.d. – not determined.

of the Mt Cer ME rocks is dominated by mafic minerals (> 80 vol. %). This feature is uncommon for mafic microgranular enclaves, usually composed of both mafic minerals and feldspars (e.g. Barbarin & Didier, 1991; Qin *et al.* 2009). Mafic microgranular enclave mineralogical composition depends on the bulk compositions of mafic and felsic end-members and the extent of their chemical interaction. Enclaves derived by subtle chemical interactions are poorly evolved and richer in mafic minerals, so they are compositionally closer to the mafic end-member. In this context, ME rocks from Mt Cer cannot represent the mafic end-member of any magma interaction process because such large amounts of mafic minerals are uncommon for mafic compositions of calc-alkaline (*sensu lato*) rocks, such as non-cumulitic gabbros and diorites (e.g. Blundy & Sparks, 1992). Poikilitic texture is common in some Mt Cer ME rocks, although clear cumulitic textures with cumulus and intercumulus phases are rare.

Compositions of amphibole and biotite from the enclaves differ from those shown by these minerals from the host (Table A1; online Appendix at http://journals.cambridge.org/geo). This is very unusual for enclaves and hosts derived by magma interaction processes because the mechanical interaction and predominant diffusion between the two magmas tend to reduce compositional differences of the mineralogical phases (e.g. Pe-Piper, 2007).

Chemical compositions of the Mt Cer ME rocks vary greatly. For instance, the enclave with the lowest silica content (113a) has similar or even lower concentrations of compatible elements in comparison to the silica-rich enclaves. This indicates that the Mt Cer ME cannot be considered as having crystallized from liquids. In addition, the ME and QMZD define clear geochemical trends only for a few elements. The geochemical trends defined by MME and their hosts are controlled by relative compositions of end-members and by bulk partition coefficients (e.g. Poli & Tommasini, 1991; Elburg, 1996; Karsli *et al.* 2007). Compatible element contents in typical MME and hosts usually form continuous trends, but this is not the case for the Mt Cer ME and QMZD.

All these findings support the hypothesis that the Mt Cer ME have a cognate origin, that is, that they likely represent clusters of fractionated phases that formed during the evolution of the QMZD magmas, rather than mafic microgranular enclaves. By contrast, the large enclave found in the southern part of the pluton may represent a MME because it has a typical MME mineralogical assemblage. This suggests that magma interaction processes might have had some role, even if a minor one, in the genesis of QMZD.

It is commonly accepted that textures such as boxy cellular crystals, oscillatory zoning, calcic spike zones and combinations of these within individual plagioclase crystals are indicative of disequilibrium crystallization (Hibbard, 1995). Such textures are interpreted as having formed in a dynamic magmatic environment, which

https://doi.org/10.1017/S0016756810000476 Published online by Cambridge University Press

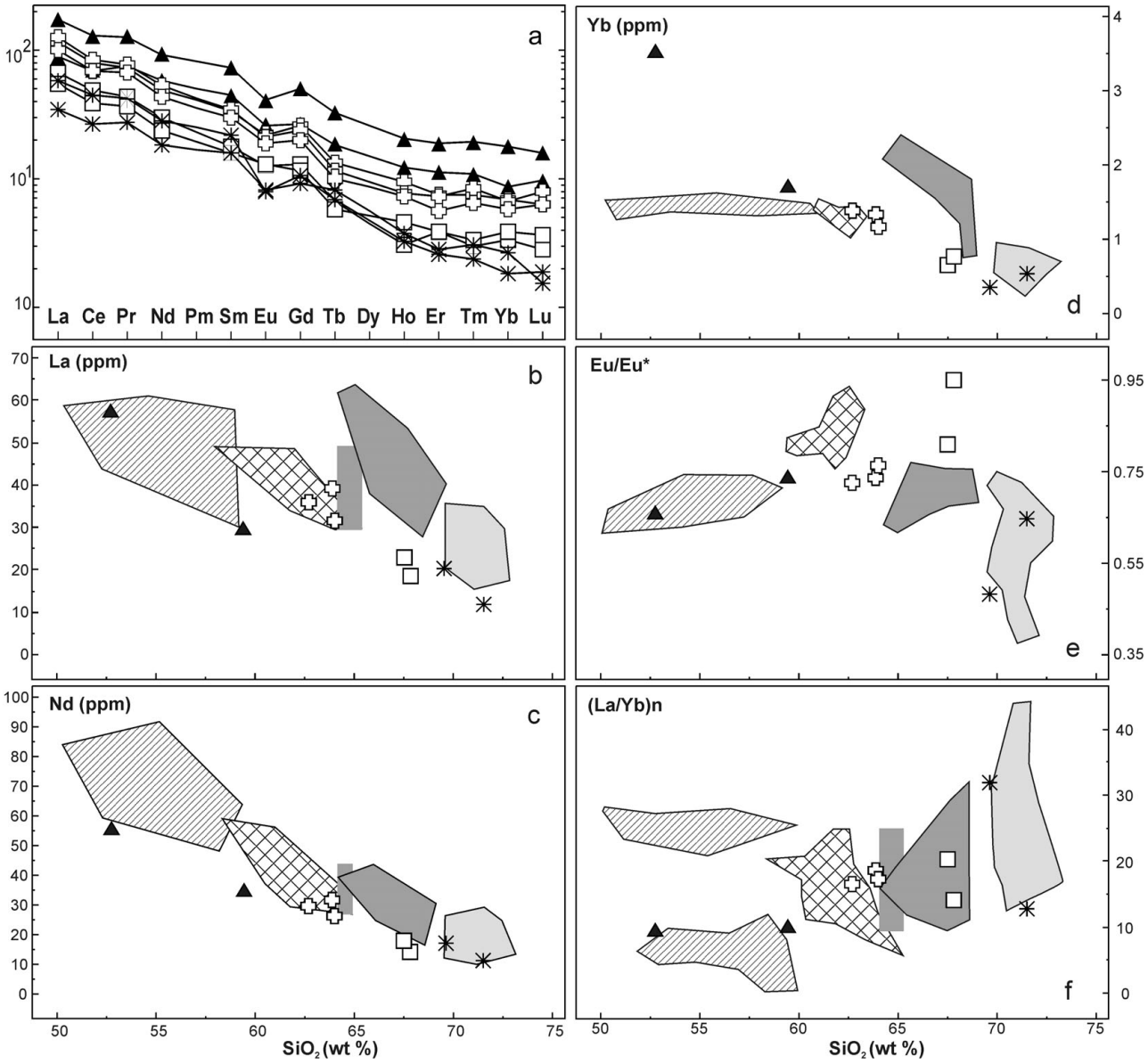

Figure 5. Chondrite normalized REE patterns (chondrite values from Haskin *et al.* 1966), La, Nd, Yb, $(La/Yb)_n$, and Eu/Eu* v. SiO_2 for the Mt Cer plutonic rocks, H-BG and TMG rocks from the Mt Bukulja pluton (Cvetković *et al.* 2007), as well as dacites and minettes/leucominettes from Veliki Majdan (Prelević *et al.* 2004). Symbols as in Figures 3 and 4.

facilitated magma interaction on a variety of scales and at different stages between the source and the emplacement levels. However, such a direct evidence of magma interaction is missing in the QMZD and ME rocks, indicating that such a process cannot be invoked as the main process responsible for the genesis of QMZD.

Chemical variability of QMZD, albeit not very large, could be explained by aqueous transport of chemical elements (Alderton, Pearce & Potts, 1980; Kirschbaum *et al.* 2005). This hypothesis can be ruled out, however, because the studied rocks and minerals are completely fresh and they lack common alteration products (e.g. sericite, chlorite etc). The observed variations might have been produced if QMZD had strongly interacted with exceptionally REE-rich fluids, but such fluids were missing in the Mt Cer pluton.

Another important issue is the compositional similarity between QMZD rocks and dacites of the Veliki Majdan area (Figs 4–7) that could suggest a similar genesis. In addition, the variation trends and REE patterns given in Figures 4 and 5 show that the Veliki Majdan dacites and QMZD rocks plot between minettes/leucominettes and GDS rocks. This suggests that the dacites and QMZD may have originated by evolutionary processes starting from minettes/leucominettes and/or by interaction processes between minettes/leucominettes and GDS-like magmas.

A closed-system crystal fractionation starting from any given basic magma from the Veliki Majdan area (Prelević *et al.* 2004) cannot be the model for QMZD origin and evolution because of variable isotopic compositions. Fractional crystallization coupled with

https://doi.org/10.1017/S0016756810000476 Published online by Cambridge University Press

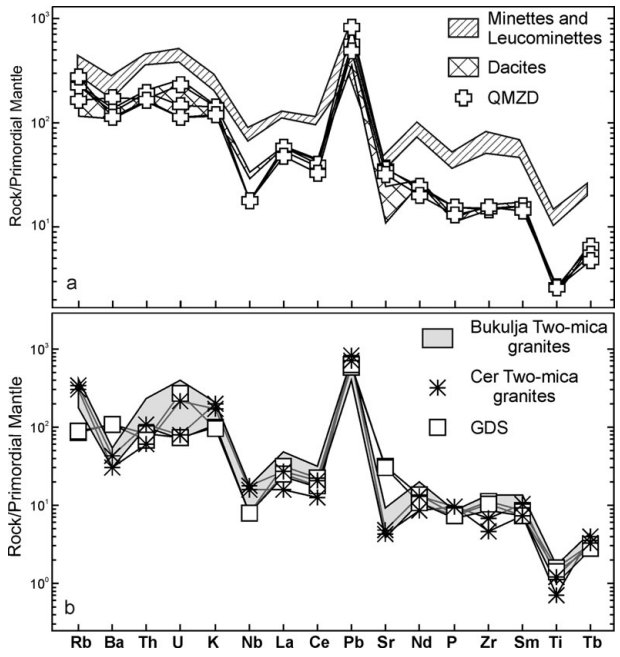

Figure 6. Primitive mantle-normalized multi-element spider diagrams for QMZD in comparison to dacites and minette/leucominettes from Veliki Majdan (a), and for GDS and TMG in comparison to Mt Bukulja two-mica granites (b). Data for dacites and minettes/leucominettes are from Prelević *et al.* (2004). Data for Bukulja two-mica granites are from Cvetković *et al.* (2007). Normalization values for primordial mantle are from Wood *et al.* (1979), but for Pb from McDonough *et al.* (1992). Symbols as in Figures 3 and 4.

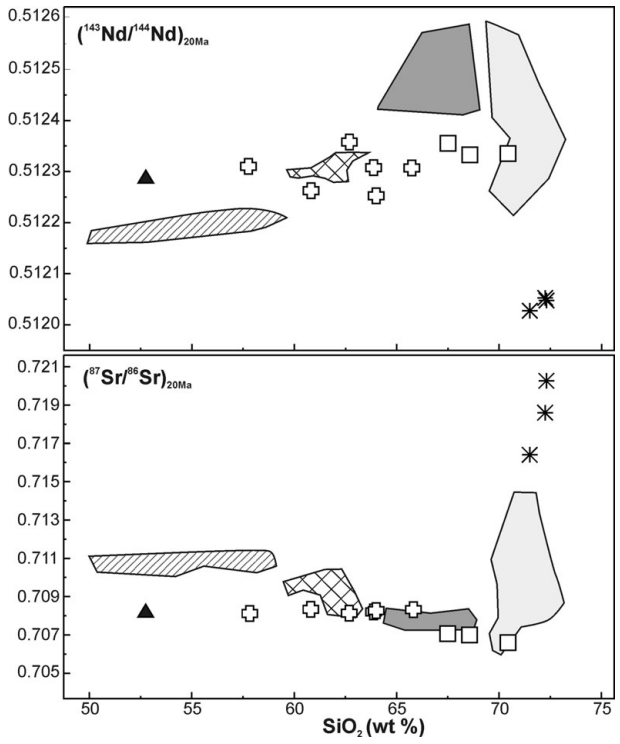

Figure 7. SiO_2 (wt %) v. $(^{87}Sr/^{86}Sr)_{20Ma}$ and $(^{143}Nd/^{144}Nd)_{20Ma}$ for the Mt Cer plutonic rocks. H-BG and TMG rocks from Bukulja pluton (Cvetković *et al.* 2007) as well as dacites and minettes/leucominettes from Veliki Majdan (Prelević *et al.* 2004). Symbols as in Figure 3.

assimilation (AFC process; De Paolo, 1981) can explain the variability in isotopic composition, but QMZD rocks have a less crustal-like Sr–Nd isotopic signature (lower $^{87}Sr/^{86}Sr$ and higher $^{143}Nd/^{144}Nd$) in comparison to the Veliki Majdan basic rocks (minettes/leucominettes). Thus a possible contaminant must have very peculiar isotopic compositions, with $^{87}Sr/^{86}Sr$ lower than 0.707 and $^{143}Nd/^{144}Nd$ higher than 0.5124, and crustal rocks with such isotopic compositions are unknown in the area.

An alternative hypothesis could be a model of mixing plus fractional crystallization (MFC; e.g. Wei, Congqiang & Masuda, 1997; Poli & Tommasini, 1999; Janousek *et al.* 2004; Gagnevin *et al.* 2007), with a mathematical formulation analogous to AFC (De Paolo, 1981). A reasonable approximation for the felsic end-member could be the composition of GDS rocks, whereas an average composition of minettes/leucominettes from the Veliki Majdan area could be a proxy for the mafic end-member. Results of the MFC modelling are presented in Figure 8a, b, showing the variation of $^{87}Sr/^{86}Sr$ initial ratio versus Sr contents and $^{143}Nd/^{144}Nd$ initial ratio versus Nd contents, respectively. In the model for Sr isotopes (Fig. 8a), two lines of descent are calculated by varying the values of r (ratio rate of assimilation over rate of crystallization) and D^{Sr} (bulk partition coefficient) in the De Paolo (1981) equations until a best fit is achieved encompassing the observed variability. The two lines of descent bound a set of models with intermediate D^{Sr} values. The results show that the MFC modelling could be considered satisfactory for explaining the petrogenesis of QMZD rocks, even if the calculated values of degree of fractionation are quite high, about 58 % and 60 % for the two lines of descent. The lines of descent calculated using values of the r parameter smaller than 0.5 would require an unrealistically high degree of fractionation (> 0.9). The same procedure has been applied for $^{143}Nd/^{144}Nd$ (Fig. 8b) and the results show that the MFC process cannot encompass the observed variability, and that using $r < 0.5$ values produces even worse results.

It is known that a clear dichotomy exists in the geochemical behaviour of isotopes and trace elements during magma interaction processes, due to sharp differences in diffusion rates. Namely, the isotope diffusion is more than one order of magnitude faster than the trace element diffusion (e.g. Waight, Maas & Nicholls, 2001; Christofides *et al.* 2007). We therefore tried to model the MFC process using trace elements alone. We modelled the lines of descent for 11 elements using Cr contents as the differentiation index. In Figure 8c the plot of Cr versus Rb is reported as an example, and in Table A2 (online Appendix at http://www.cambridge.org/journals/geo) the modelled bulk partition coefficients for all elements are reported. We also calculated the felsic/mafic ratio for each QMZD rock (parameter ρ from Aitcheson & Forrest, 1994, equation 6; Table A2), and we report ρ values for QMZD rocks in Figure 8d. The ρ values for each rock

https://doi.org/10.1017/S0016756810000476 Published online by Cambridge University Press

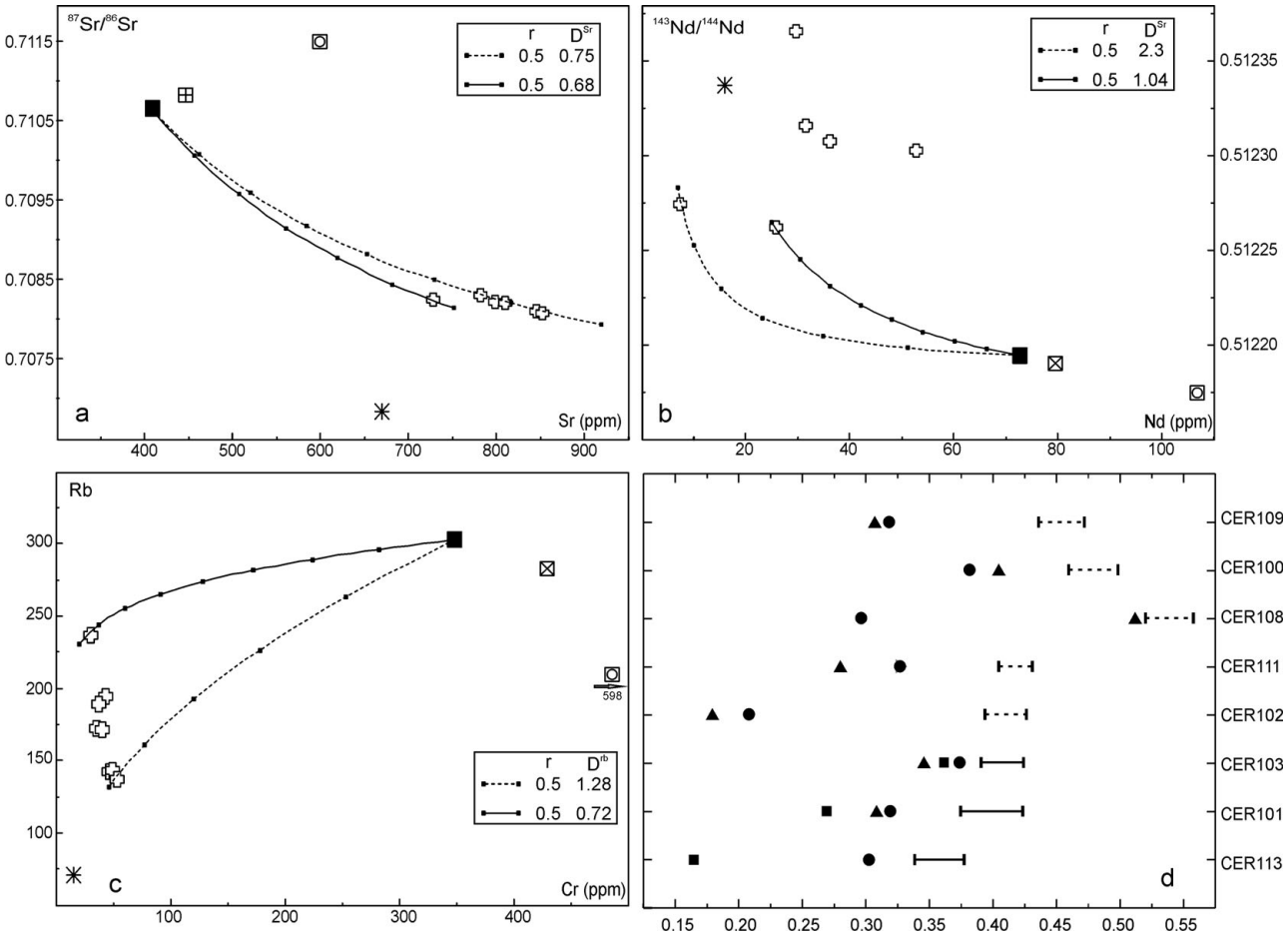

Figure 8. $(^{87}Sr/^{86}Sr)_{20Ma}$ v. Sr (a), $(^{143}Nd/^{144}Nd)_{20Ma}$ v. Nd (b), and Cr v. Rb (c) diagrams showing the best fit of two MFC lines needed to encompass the variability of composition of the QMZD rocks. Solid square – mafic end-member, average composition of minettes/leucominettes from Veliki Majdan. Star – felsic end member, average composition of GDS rocks. Open square with cross – average composition of minettes, leucominettes, and lamproites. Open square with circle – average composition of lamproites. All mafic magmas from Prelević *et al.* (2004). Tick marks are reported at 10 % intervals of crystal fractionation; r – rate of mixing over rate of fractional crystallization; D – bulk partition coefficient. Other symbols as in Figure 3. (d) Values of felsic/mafic magma ratios ρ for each QMZD sample and selected elements as calculated using equation 6 from Aitcheson & Forrest (1994) for MFC process whose parameters are reported in the text. Solid segment – variation of ρ for Cr, Rb, Sr, Zr, and Nb; dashed segment – variation of ρ for the previous elements and La, Nd, Tb, and Th; solid triangle – Ba; solid circle – Y; solid square – Yb.

should be the same for all the elements if the modelling is correct. Although the ρ values are fairly constant for some elements, they are extremely variable for Ba, Y and Yb. This indicates that the MFC process cannot reproduce the variability of QMZD rocks even if we use only trace element concentrations in modelling. It could be suggested that using different mafic and felsic magmas the MFC model could give better results. The compositions of some different possible mafic magmas are reported in Figure 8a–c. It is evident that the modelled results would be even worse for $^{143}Nd/^{144}Nd$, due to the higher values of elemental Nd in these mafic magmas, and the same holds for trace elements. For instance, adopting mafic magmas with Cr contents higher than those from the minette/leucominette basic end-member would produce even higher calculated degrees of fractionation. On the other hand, TMG is the only other candidate in the area for representing the composition of the felsic end-member. However, $^{87}Sr/^{86}Sr$ initial ratios and Sr contents must decrease in the model in order to encompass the compositional variability of QMZD rocks and this is not possible using TMG compositions (De Paolo, 1981). In conclusion, isotope and trace element geochemistry suggests that MFC is not a likely process for generation of QMZD rocks. This is corroborated by the lack of MME and by the absence of disequilibrium textures in minerals (e.g. Chen, Chen & Jahn, 2009).

Given that the QMZD rocks plot between minettes/leucominettes and GDS rocks on many variation diagrams, a simple two end-member mixing process could be proposed. Actually, Prelević *et al.* (2004) argued that dacites (similar to QMZD in composition) are petrogenetically related to the minette/leucominette rocks, and that the leucominettes are produced by two end-member mixing between a lamproite melt and dacites, although little is said about the genesis of the dacites (e.g. fig. 12 from Prelević *et al.* 2004). It is worth noting that Prelević *et al.* (2004) found many disequilibrium textures but only in the leucominettes

https://doi.org/10.1017/S0016756810000476 Published online by Cambridge University Press

and not in the dacites. Furthermore, they did not find MME in either the leucominettes or the dacites, and they found dacite-derived mineral phases in the leucominettes, but no leucominette-derived mineral phases were found in the dacites.

In order to constrain the simple two end-member mixing process, we applied the binary mixing test of Fourcade & Allègre (1981). We used the average GDS composition to represent the acid magma composition (C_a), the average composition of minettes/leucominettes to represent the basic magma (C_b), and the average composition of QMZD rocks (C_{qmzd}) to represent the mixed magma. The plot ($C_b - C_a$) versus ($C_{qmzd} - C_a$) should give a straight line with its slope ranging between 0 and 1 and representing the mass proportions of C_a in the mixture. The fitted line (not shown) calculated using all the elements reported in Tables 2 and 3 has a slope of 0.76 with a $R^2 = 0.82$. These results seem reasonable at first glance, but we need to consider the so-called 'King Kong effect' which often occurs when elements with strongly different concentrations are used (Makridakis, Wheelwright & Hyndman, 1998, chapter 5). Namely, extreme observations can influence linear correlation between variables masking a deceiving correlation, and acting such as goodness of parameters (e.g. sum of the squared deviations) can be misleading. To overcome this effect we plot the slopes of each element against elements; if correlation is correct all the elements should have the same slope, and this is not the case, as shown in Figure 9a. Moreover, some slopes are outside the permitted values (0–1). It could be argued that using the average composition for QMZD rocks as reflecting the composition of hybrid magma, the correlation could be lost. Therefore, we performed calculations using the composition of every single QMZD rock as reflecting the composition of hybrid magmas, and we report minimum and maximum slope values in Figure 9a. It is evident that all the elements cannot be taken into account for each QMZD sample as the result of a two end-member magma mixing process.

We plotted major and trace element ratios versus Zr concentrations following figure 12 of Prelević *et al.* (2004), and some plots are reported in Figure 9b–d. Some elements plot very close to simple binary mixing hyperbolae (e.g. SiO_2, Fig. 9b) and their companion plots, against 1/Zr, plot close to the line, indicating that such elements can be modelled by a magma-mixing process (Langmuir *et al.* 1978). Plots of other elements (e.g. La and Yb, Fig. 9c, d) differ from simple binary mixing hyperbolae and lines, indicating that they cannot be modelled by two end-member mixing. We calculated the correlation coefficients (R^2) for all the elements for the companion plots. SiO_2 and Al_2O_3 perfectly follow two end-member mixing trends (0.997 and 0.995), whereas Sr and Rb do not (0.84 and 0.56). LREE plots are strongly scattered ($R^2 = 0.60$) in comparison to HREE ($R^2 = 0.87$).

We believe that such differences in element behaviour give a clue to the genesis of QMZD. Because these differences cannot be due to specific fractionating mineral assemblages (see above), it can be supposed that they resulted from different diffusion coefficients. As general rule, major elements have the lowest diffusion coefficients ($\sim 10^{-13}$ cm^2/sec; e.g. Liang, Richter & Watson, 1996), whereas Rb and Sr have the highest diffusion coefficient ($\sim 1.7^{*}10^{-7}$ cm^2/sec at 1500 MPa; Nakamura & Kushiro, 1998). In addition, LREE have higher diffusion coefficients (La: $1.1^{*}10^{-8}$ cm^2/sec at 1500 MPa; Nakamura & Kushiro, 1998) than HREE (Lu: $7^{*}10^{-8}$ cm^2/sec at 1500 MPa; Nakamura & Kushiro, 1998). These findings imply that diffusion played an important role in the petrogenesis of QMZD, and that diffusion was probably controlled by specific conditions during magma interaction processes. When a felsic magmatic mass overlies a mafic one, the two magmatic masses tend to remain separated at the very beginning, because of the density contrast, but this does not preclude chemical exchanges taking place. As stated by Snyder & Tait (1998) and Christofides *et al.* (2007), a convection–diffusion process could influence the concentration of isotopes and elements having the highest diffusivity. $^{87}Sr/^{86}Sr$ and $^{143}Nd/^{144}Nd$ have the highest diffusion coefficients (e.g. Lesher, 1990), whereas these coefficients are progressively lower for trace and major elements, the latter displaying the lowest diffusivity (e.g. Waight, Maas & Nicholls, 2001). The reason for this behaviour lies in the fact that diffusion of major elements is controlled mostly by diffusivity of Si and Al, which are network-forming cations. This means that these elements may diffuse only by restructuring the melt, which is difficult to achieve. On the other hand, diffusion of isotopes and trace elements does not require the melt restructuring and, therefore, the mobility of these elements in the melt is much higher. Quartz monzonite/quartz monzodiorite rocks have geochemical characteristics such that major element contents, particularly SiO_2 and Al_2O_3, perfectly follow two end-member mixing trends (Fig. 9b), whereas trace element (Fig. 9c, d) contents and isotope ratios (Fig. 7) show a lot of scatter. During magma interaction processes, diffusion is further enhanced by convection in each of the two magmas caused by their thermal differences. This process of convection–diffusion may thus change the chemical composition in the felsic magma even in the overt absence of mixing.

During such processes, thermal and rheological contrasts between the mafic magmatic mass and the overlying felsic one are progressively smoothed. These new conditions change the nature of interaction in which magma mixing becomes more important and higher efficiency of mixing is enabled (e.g. Sparks & Marshall, 1986; Poli, Tommasini & Halliday, 1996).

The above discussion suggests a scenario for the formation of QMZD in which a felsic magmatic mass having composition similar to GDS rocks was overlying a mafic magmatic body similar in composition to minettes/leucominettes. At the beginning, a convection–diffusion process influenced the elements

https://doi.org/10.1017/S0016756810000476 Published online by Cambridge University Press

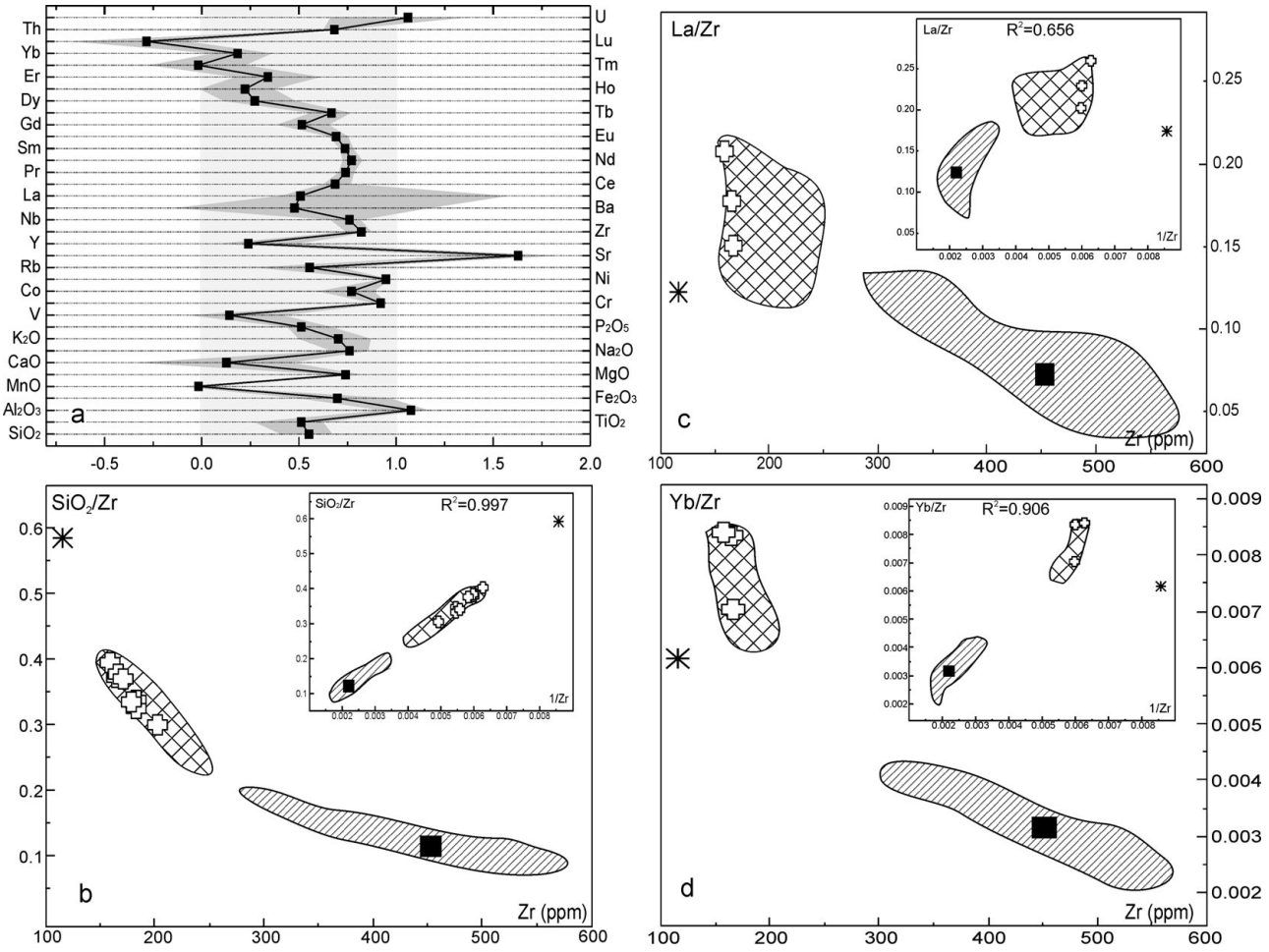

Figure 9. (a) Binary mixing test of Fourcade & Allègre (1981) for elements reported in Tables 2 and 3 using: the average composition of GDS rocks as acid magma composition, the average composition of minettes/leucominettes as reflecting the basic magma composition, and the average QMZD rocks to represent the mixed magma. Value of each closed square represents the mass proportions of acid magma in the mixture for each element. Dark grey field represents minimum and maximum of mass proportions of acid magma in each QMZD rock, considered as a mixture, for each element. Light grey rectangle is the field of permitted values for the proportions of acid magma according to Fourcade & Allègre (1981). Selected major element oxide (b) and trace element ratios (c, d) v. Zr. In the insets, companion plots v. 1/Zr are reported. Data for dacites, and minettes/leucominettes are from Prelević *et al.* (2004).

of the highest diffusivity. In such a way, the GDS magma was driven to change the concentrations of Sr, Rb and REE, but not the contents of major elements. When the contrasts in composition between the two magmas decreased, a simple two end-member mixing occurred, causing a change of the concentrations of all the elements. In this way the elements not affected by the convection–diffusion process followed a clear two end-member mixing trend (Fig. 9b), whereas those modified by this process have scattered trends (Fig. 9c, d). The lack of mafic microgranular enclaves and disequilibrium textures in mineral phases in the produced melts (QMZD and dacites) is consistent with the proposed scenario. Namely, the mafic magma acted only as a chemical contaminant during the convection–diffusion process, whereas an almost complete two end-member mixing excluded the possibility of disequilibrium textures being produced or physical dispersion of magmas into each other. However, the process itself does not completely preclude having a few larger mafic microgranular enclaves, such as that found in the southern part of the pluton.

The scenario outlined above is different from many interpretations of mixing processes (e.g. Bateman, 1995; Karsli *et al.* 2007). The explanations could be found in the fact that this convection–diffusion process followed by two end-member magma mixing occurred at pressures higher than 600 MPa, as suggested by an amphibole geobarometer and by the presence of weak thermal metamorphism effects at the emplacement level of QMZD. From 30 Ma to 15 Ma, basaltic (*sensu lato*) magmatism took place in the intermediate/lower crust (e.g. Cvetković *et al.* 2004; Prelević *et al.* 2005) causing an increase of isotherms in the area and providing conditions for partial melting of intermediate and lower crust (see below; e.g Annen, Blundy & Sparks, 2006). Perugini & Poli (2005) showed that the initial stages of magma interaction, when the mafic magma enters the felsic magma chamber, are governed by viscous fingering dynamics. The morphology of interfaces between mafic and felsic magma depends on relative viscosity. At low viscosity ratios, the interface is roughly plain, preventing fountain-like interactions and effective mixing. At high viscosity

https://doi.org/10.1017/S0016756810000476 Published online by Cambridge University Press

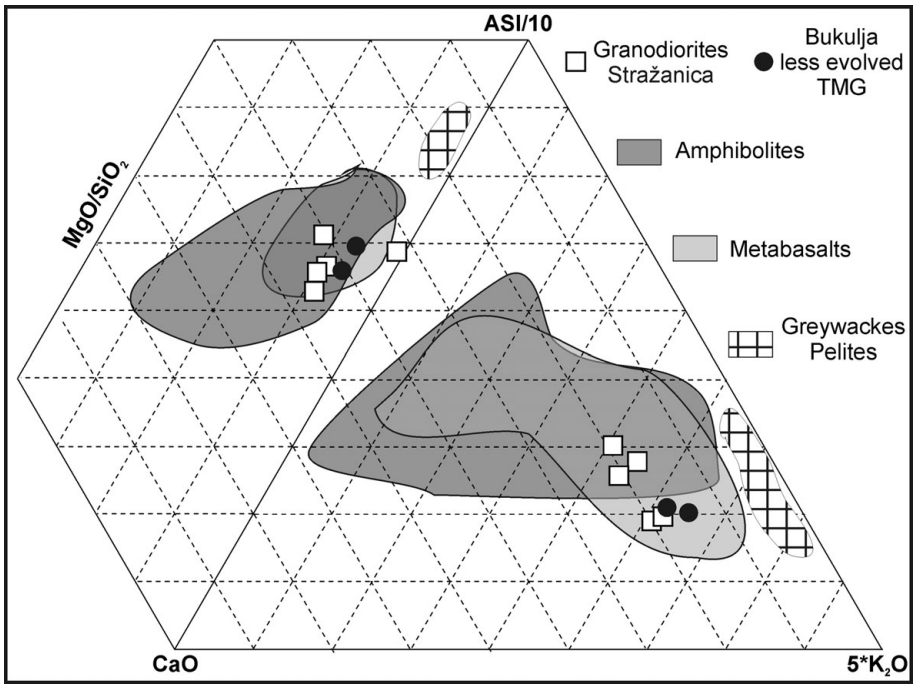

Figure 10. ASI/10–CaO–5*K_2O (molar), and ASI/10–CaO–MgO/SiO_2 (molar) triangular diagrams displaying the composition of the GDS rocks compared with experimental data of melt compositions from different crustal protoliths at 1500 MPa. References for the various sources are reported in online Appendix at http://journals.cambridge.org/geo.

ratios, finger-like patterns are generated and they usually enhance mixing processes between the low-viscosity mafic magma and the high-viscosity felsic magma. The viscosity ratio for the two interacting magmas in the proposed model has been calculated assuming different crystal percentages and pressure of 2000 MPa (Shaw, 1972; Bottinga & Weil, 1972). Under the worst conditions, that is, with a crystal-free mafic magma and 50 % crystallized felsic magma, the viscosity ratio is only about 3×10^2. On the other hand, the high temperature in the area would depress nucleation and crystallization of magmas, and would increase temperature in the felsic magma, so the viscosity ratios would be even lower, prohibiting extensive magma mixing (see fig. 4 of Perugini & Poli, 2005). This supports the hypothesis that initial hybrid QMZD magmas may have resulted mainly from convection–diffusion rather than magma-mixing processes, whereas the latter processes subsequently became more important.

Once the QMZD magmas formed, they ascended and were emplaced, producing a weak contact metamorphism. They started to crystallize at about 500 MPa, and continued to ascend up to 300–400 MPa according to pressures reported in Figure 3b. Cognate ME started to be generated at about 500 MPa with maximum formation at about 400 MPa and 200–300 MPa (Fig. 3b). The nearly continuous pressure of formation of QMZD and ME was caused by uplift and erosion during the opening of the Pannonian Basin. The age of these processes can be constrained by data reported in Table 1. Quartz monzonite/quartz monzodiorite magmas were emplaced earlier than *c*. 21 Ma, and a minimum age of this emplacement is obtained on hornblende. The final crystallization of QMZD magmas probably occurred earlier than *c*. 17 Ma, assuming that the K/Ar age data on biotites represent the cooling age. The above considerations suggest that a time span between the emplacement and final crystallization of QMZD was about 4 Ma. During this time the QMZD body was continuously ascending. Assuming blocking temperatures for ^{40}K–^{39}Ar of amphibole and biotite of 500–600 °C and 300–350 °C, respectively, the pluton cooled at a rate of about 40–75 °C/Ma. Such a rate is consistent with calculated rates from various plutons (e.g. Pitcher, 1997, chapter 12; Long, Castellana & Sial, 2005).

4.b. GDS

The Stražanica granodiorite/quartz monzonite rocks show silica contents ranging between 67.5 and 70.5 wt % and are characterized by the least crustal-like Sr–Nd isotopic signature among all the Mt Cer rocks. This indicates that they cannot be products of low-pressure processes of evolution starting from any of the less evolved magmas present in the area. Besides, the above discussed origin of QMZD implies that GDS originated by partial melting of intermediate/lower crust. The relatively low Sr and high Nd isotopic ratios strongly narrow the possibility that GDS rocks originated by partial melting of upper crustal rocks, unless a very young upper crust is involved, for which there is no geological evidence (e.g. Cvetković *et al.* 2007). In addition, GDS are mainly metaluminous or slightly peraluminous rocks, and this excludes an Al-rich crust as a potential source. In Figure 10 the composition of GDS rocks is plotted along with data of melt compositions obtained by melting experiments

https://doi.org/10.1017/S0016756810000476 Published online by Cambridge University Press

Table 5. Range of trace element abundances in GDS rocks and source used in the partial melting model

	CER-GDS			Source	Modelled bulk partition	Partition coefficients used in the model							
	Average	Min	Max	arc-andesite*	coefficients	Amp	Cpx	Pl	Bt	Grt	Ap	Zrn	Spl
Rb	70	61	78	46	0.51	0.18	0.1	0.01	4.1	0	0.4	0	0.008
Sr	648	539	735	587	0.88	0.49	0.37	3	0	0	9.2	0	0.52
Ba	690	433	827	501	0.61	0.82	0.14	0.5	1.5	0.02	0.5	0	0.014
Th	7.2	6.6	7.8	4.51	0.47	0.45	0.1	0.01	1.1	0	4.6	0	0.54
Nb	5.3	5	6	8	1.64	1.5	0.6	0.025	0.09	0.05	0	0	39
Y	6.7	6	8	17	3.03	0.017	1	0.06	0.01	52	21	500	0.08
Zr	116	113	122	587	0.88	0.49	0.37	3	0	0	9.2	0	0.52
La	20.1	18	22.3	19	0.92	0.44	0.2	0.03	0.7	0.37	21.1	17	0
Ce	38.2	34	42.3	37	0.95	0.63	0.48	0.22	0.05	0.53	16.9	17	0.73
Nd	16	14.1	18	21	1.44	1.3	0.7	0.15	0.04	0.81	22	13.3	0.28
Sm	3.05	2.84	3.26	3.9	1.38	0.66	1	0.1	0.03	5.5	21	14.4	0
Eu	0.88	0.87	0.9	1.08	1.32	0.36	1	2	0.03	1.37	22	16	0
Tb	0.29	0.28	0.31	0.51	2.11	1.5	1.45	0.04	0.04	16	15	25	0.008
Yb	0.72	0.66	0.77	1.5	2.54	1.31	1.4	0.041	0.04	29	12	300	0.009
Residual minerals %						43	29.3	9.8	9.6	3.6	2.7	0.1	1.9

*Data for source are from Kelemen *et al.* (2007). Bulk partition coefficients used to model GDS rocks. Residuum assemblages calculated using linear programming (Wright & Doherty, 1970) minimizing the sum of squares of residuals as a constraint (SSR). Mineral abbreviations are after Kretz (1983).

of various crustal protoliths. The graph shows that GDS samples are compositionally similar to the melts derived from metabasalts and amphibolites, and depart from those produced by melting of greywackes and pelites.

Melts with major-element compositions similar to GDS rocks can be produced by fluid-absent partial melting of metabasaltic rocks under a wide variety of conditions (e.g. Clemens, 2006). Many authors have studied pressure and temperature ranges, and residual assemblage of partially melted amphibolites and coexisting residual phases (e.g. Sen & Dunn, 1994; Rapp & Watson, 1995; Clemens, Yearron & Stevens, 2006). Garnet can be considered stable at $P \geq 1.5$ GPa, and its stability is mostly temperature-independent, whereas the amount of garnet in the restite is controlled by both temperature and presence of plagioclase in the protolith. At pressures $P \geq 1.5$ GPa (garnet is present), the modal amphibole/clinopyroxene ratio in the residuum mainly depends on temperature, chemical composition, and mineral assemblage of the protolith.

Fractionated HREE (Fig. 5), and low absolute concentrations of Yb and Y in GDS rocks (Table 2) strongly suggest that garnet was present as a residual phase in the source of GDS magmas, and this implies pressures higher than 1.5 GPa. Relatively high Ba/Th ratios ($\sim$ 115; Fig. 6) are not consistent with the only presence of residual amphibole in the source, due to the preferential retention of Ba in amphibole. Hence, both amphibole and clinopyroxene must have been present as residual phases. High contents of Sr and weak or no Eu-anomaly indicate that plagioclase was not an important restitic phase. Consequently, a residual assemblage composed of amphibole + clinopyroxene + garnet $\pm$ plagioclase was likely left behind during the partial melting process that generated GDS magmas. The contents of other trace elements provide some additional constraints on the residuum mineralogy. The presence of negative Ta–Nb, P and Ti anomalies (Fig. 6), for instance, is consistent with the presence of residual rutile and apatite.

To evaluate whether partial melting of an amphibolitic source leaving behind such a residuum is a likely explanation for the petrogenesis of GDS, trace element modelling has been applied. We used subduction-modified lower crust having the average composition of more mafic (Mg no. > 60) continental andesites (Kelemen *et al.* 2007) to represent the composition of the lower crust in the northern Dinarides (Table 5). Given that the source mineral assemblage is difficult to envisage, we used the following formulation for a non-modal batch melting model (Rollinson, 1993):

$$C_l = \frac{C_0}{D_r + F^*(1 - D_r)},$$

where C_0 and C_l are the concentrations of a given trace element in the source and melt, respectively, D_r is the bulk partition coefficient of the residual solid, and F is the weight fraction of melt produced.

In Figure 11 the best model is shown as a spider diagram normalized to the source for degree of melting of 0.3. There is a remarkable match for all the elements between modelled melt and GDS. Modelled bulk partition coefficients and percentages of residual minerals are given in Table 5. The percentage of residual minerals has been calculated by linear programming, minimizing the sum of squares of residuals as a constraint (SSR; e.g. Wright & Doherty, 1970) starting from the bulk partition coefficient modelled and using literature partition coefficients (Table 5; GERM data set, http://earthref.org/GERM/main.htm).

Degree of melting (F = 0.3) is consistent with the supposed presence of amphibole and clinopyroxene in the residuum (e.g. Rapp & Watson, 1995). The presence of mica is necessary to account for Rb and Ba

https://doi.org/10.1017/S0016756810000476 Published online by Cambridge University Press

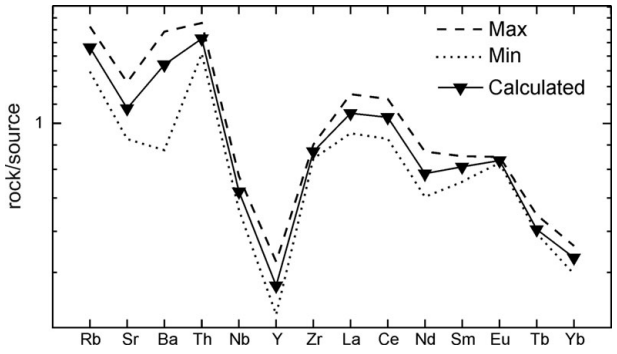

Figure 11. Source-normalized spider diagram of minimum and maximum of reported elements in the GDS rocks from Mt Cer, together with the modelled melt after 0.3 degree of melting of the Arc Andesite source reported in Table 5.

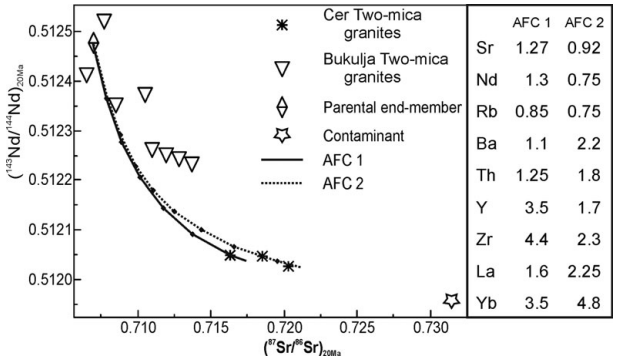

Figure 12. $(^{87}Sr/^{86}Sr)_{20Ma}$ v. $(^{143}Nd/^{144}Nd)_{20Ma}$ showing the two AFC models (AFC 1 and AFC 2) needed to encompass the variability of composition of the Mt Cer TMG. Modelled bulk partition coefficients D for Sr and Nd, and for a series of trace elements for the two models are also given. Parental end-member and contaminant are the average composition of most primitive TMG rocks and sample BK136 from the metamorphic basement, respectively. Both end-members are from the Mt Bukulja pluton (Cvetković *et al.* 2007). Tick marks are reported at 10 % intervals of crystal fractionation.

contents. A subduction-modified lower crust has higher Rb and Ba abundances relative to a MORB-like source (e.g. GERM, http://earthref.org/GERM/main.htm), and this is a further indication of the presence of residual mica. On the other hand, Rapp & Watson (1995) argued that biotite is present at 800 MPa and 1000 °C for the most potassium-rich source (N°1 alkali rich basalt, $K_2O = 0.82$ in Rapp & Watson, 1995). The source used for the present model contains double that value; it is thus reasonable to assume that mica could be a residual phase even at higher pressures. The presence of small amounts of plagioclase is consistent if melting temperature is below 1025 °C at 1600 MPa (Rapp & Watson, 1995). On the basis of the above discussion, it can be concluded that partial melting of lower crust having an average composition of mafic continental andesites can produce magmas which are geochemically similar to GDS. It is noteworthy that the presence of small amounts of plagioclase accounts also for the peculiar behaviour of Sr in QMZD (Fig. 4d). The Sr contents in melts are controlled by plagioclase, and because this phase is not strongly enriched in the restite, Sr contents in the produced GDS melt are quite high.

4.c. TMG

Two-mica granites are the most evolved rocks of the Mt Cer pluton and have a peraluminous character. In terms of mineral chemistry and major and trace element geochemistry, they are similar to the two-mica rocks from Mt Bukulja pluton, but the Mt Cer TMG have higher initial $^{87}Sr/^{86}Sr$ and lower $^{143}Nd/^{144}Nd$ isotope ratios. In Figure 12 the composition of the two-mica granites from the Mt Cer and Mt Bukulja plutons are plotted together with the composition of basement rocks. The latter were considered by Cvetković *et al.* (2007) as the contaminant in an AFC model of the evolution of the Mt Bukulja TMG. It is clear that Mt Cer TMG plot in continuity with Mt Bukulja TMG rocks, suggesting a similar evolution. Such a hypothesis has been tested using the approach of Cvetković *et al.* (2007) for a set of trace elements and the modelled bulk partition coefficients (Fig. 12). Two evolution lines are used for encompassing the TMG variability, at a constant value of r = 0.4 (De Paolo, 1981). Fractionating assemblages have been calculated by linear programming, minimizing the sum of squares of residuals as a constraint (SSR; e.g. Wright & Doherty, 1970), starting from the bulk partition coefficient modelled and using literature partition coefficients (GERM dataset, http://earthref.org/GERM/main.htm). Calculated fractionating assemblages are similar for the two models AFC1 and AFC2, and are roughly dominated by quartz (~ 40 %), plagioclase (~ 35 %), K–feldspar (~ 8 %) and biotite (~ 13 %). In comparison to the AFC model for TMG rocks from the Mt Bukulja pluton, a greater amount of feldspars is necessary to reproduce the observed geochemical trends. This is in agreement with lower mean contents of Sr in the Mt Cer TMG (100 ppm) relative to Mt Bukulja TMG (150 ppm). In addition, the increase of feldspar in the fractionating assemblage is inferred by the high Eu anomaly in the Mt Cer TMG rocks (Fig. 6). The amount of accessory minerals (apatite 1.3 %, titanite 0.25 % and zircon 0.15 %) is more or less similar for the Mt Bukulja and Mt Cer models, although more zircon and a very small amount of allanite (0.05 %) are necessary to reproduce the geochemistry of Mt Cer TMG. These slight differences may have resulted from local changes in the magma chamber and in the contaminant.

5. Geodynamic constraints

The Mt Cer pluton, along with the adjacent Mt Bukulja pluton, has a specific geotectonic position. Both plutons are situated at the junction between the southern Pannonian Basin and northern Dinarides. The foregoing discussion has shown that the Mt Cer pluton consists of I- and S- type intrusions that show

https://doi.org/10.1017/S0016756810000476 Published online by Cambridge University Press

differences in age and composition and thereby reflect important differences in their source, evolution and geodynamic conditions.

The age of the Mt Cer pluton is not completely constrained, but there is evidence that the complete consolidation of QMZD and TMG occurred not later than 17 Ma and 16 Ma, respectively, whereas that of GDS is similar to QMZD at *c.* 17 Ma. Therefore, it is very likely that the Mt Cer pluton is genetically unrelated to widespread Oligocene granitoid bodies which can be, with some gaps, traced from the Periadriatic line southeastwards (Fig. 1; e.g. Laubscher, 1983; Elias, 1998; Rosenberg, 2004). These plutons in Serbia stretch roughly NW–SE, and follow a belt of elongated Oligocene lacustrine depositional systems. These lacustrine basins are interpreted as having resulted after stabilization of the Dinaride orogen and during dextral strike-slip wrenching tectonics (e.g. Brunn, 1960; Marović *et al.* 1999, 2001). Studies of basaltic and potassic/ultrapotassic rocks from the central Balkan Peninsula (Cvetković *et al.* 2004; Prelević *et al.* 2005) imply a major role for the post-collisional orogenic collapse of the Dinarides, and such an interpretation can likely be valid for the origin of temporally and spatially related granitoid rocks. Similar processes have already been recognized in other orogenic systems (e.g. England & Houseman, 1985; Ratschbacher *et al.* 1989) where overburden gives rise to convective thinning, lithosphere instabilities and post-collisional collapse.

The Mt Cer composite pluton has an age range similar to that shown by granitoids occurring mostly along the northern Dinarides/southern Pannonian realm (e.g. Cvetković *et al.* 2007; Fodor *et al.* 2008). During the Palaeogene to Neogene tectonic regime, dominated by orogen-parallel wrenching, the final formation of a double vergent Dinaride–Carpathian–Balkan orogen occurred. The subsequent tectonic style was generally related to the formation of the Pannonian Basin. This tectonic event was combined with the Neogene indentation of the Apulian microplate which formed nap-stacking in the External Dinarides (Karamata, 2006; Schmid *et al.* 2008; Robertson, Karamata & Sarić, 2009). This is contemporaneous with, and most probably tectonically related to, the continuation of dextral orogen-parallel movements along the major axis of the Balkan Peninsula and to the extension in the Pannonian area.

Ilić & Neubauer (2005) performed a palaeostress analysis in the central Dinarides, some 200 km south of Belgrade. They reported mainly NW-trending Neogene normal faults, which indicate Early/Middle Miocene NE–SW extension related to syn-rift extension in the Pannonian basin. This suggests that the events genetically related to the Pannonian extension can be traced southwards deep in the Dinarides and that they are more apparent along their northern margin.

Our study revealed that the composite Mt Cer pluton originated after complex and multistage magmatic events involving melting of intermediate–lower crustal protoliths and evolution through convection–diffusion, magma mixing and AFC processes. It is suggested that the origin and evolution of QMZD and GDS occurred at the base of the continental crust. The present-day thickness of the continental crust across the Vardar suture is estimated at about 30 km (Aljinović, 1987). However, straddling the Oligocene–Miocene boundary the continental crust must have been relatively thicker, reaching $\sim$ 50 km, corresponding to pressures as high as 1700 MPa, having been subsequently reduced during the Dinaride wrenching and even more during the Middle Miocene Pannonian extension. Partial melting at such depths could have produced GDS-like magma that interacted with underlying minette-type magma by a convection–diffusion process. The peraluminous character and the AFC-dominated evolution of TMG imply a progressively more important role of higher levels of continental crust in the succession of these tectonomagmatic events. A significant age difference between QMZD, which started to crystallize deep in the crust, and TMG which shows sharp intrusive contacts with the former, indicates that the origin and evolution of the composite Mt Cer pluton is related to an increase of regional heat flow. This is consistent with a transition from a dextral transpression–transtension, at the beginning of Miocene times, to a normal fault-dominated tectonic style, which occurred around 4–5 Ma later.

Schematic cross-sections of the mantle–crust transition along the southern margin of the Pannonian Basin in northern Serbia during Tertiary times are shown in Figure 13. Underplating of mantle-derived magmas with high-K calc-alkaline to ultrapotassic affinities started at *c*. 35 Ma (Fig. 13a) and continued up to the end of Oligocene and beginning of Miocene times (e.g. Prelević *et al.* 2005). The underplating produced high heat flow in the lower crust that was able to induce partial melting of amphibolitic/andesitic lower crust and production of GDS-like magmas. According to our model, such magmas were underlain by minette/leucominette-like magmas (Fig. 13b). This contact first led to a convection–diffusion process influencing elements of high diffusivity, such as Sr, Rb, La and Th, but not the major elements. When the contrasts in physical parameters between the two magmas decreased, a simple two end-member mixing occurred, producing QMZD-like magmas (Fig. 13c). Such magmas were emplaced at crustal levels corresponding to about 500 MPa, where they started to crystallize producing weak thermal metamorphism (Fig. 13d). Simultaneously, some cognate mafic enclaves were formed. The Pannonian extension caused erosion events in the marginal areas, with the consequence that QMZD was uplifted to 300–400 MPa, where it continued to crystallize and finally solidified (Fig. 13e). In the meantime, a predominance of cognate enclaves formed and batches of GDS-like magma were emplaced at the same crustal level, causing strong contact-metamorphic effects (Fig. 13e). Further opening of the Pannonian Basin caused decompressional partial

https://doi.org/10.1017/S0016756810000476 Published online by Cambridge University Press

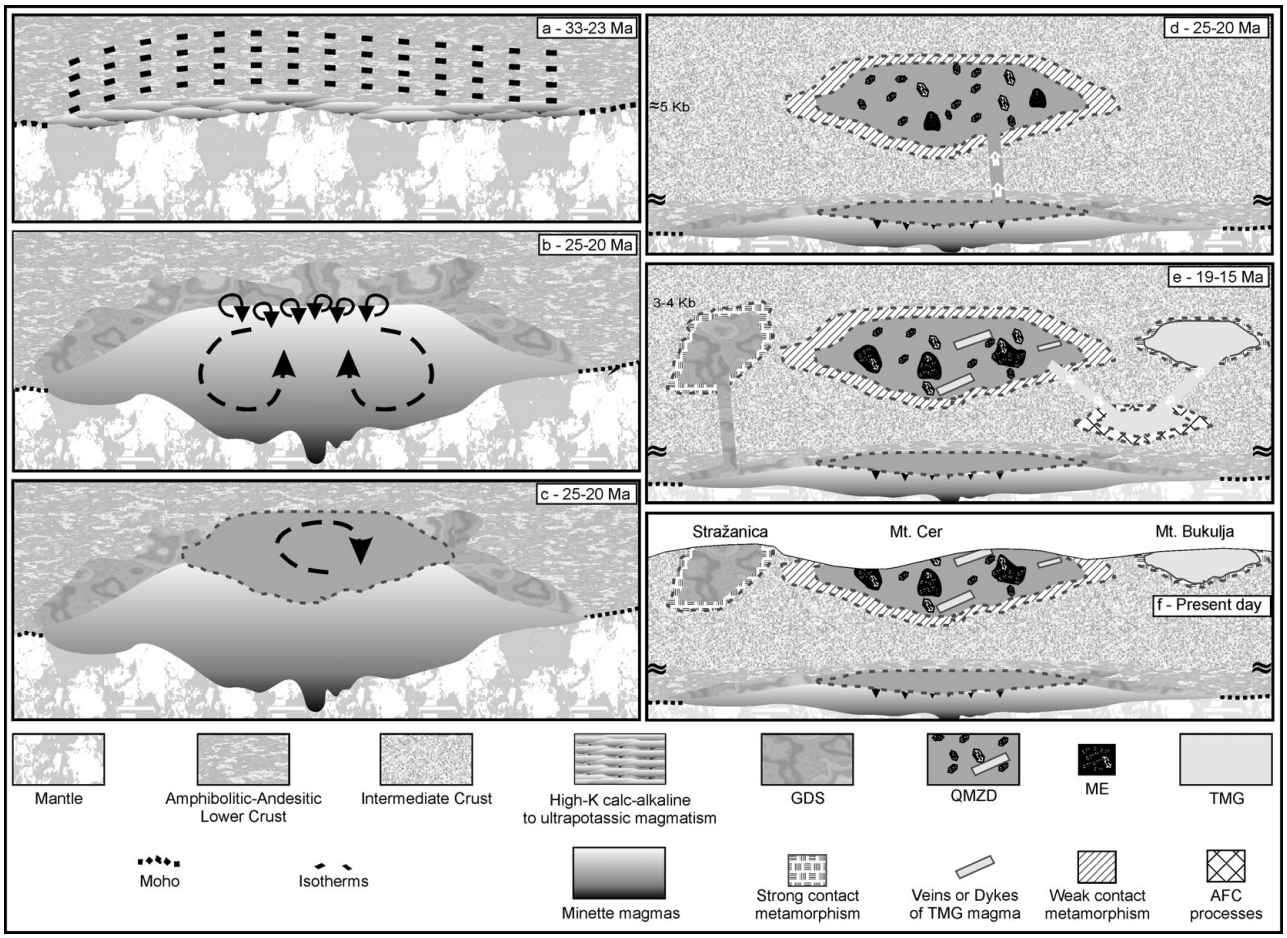

Figure 13. Schematic cross-sections of the mantle–crust transition along the southern margin of the Pannonian Basin in northern Serbia during Tertiary times, showing episodes of underplating, partial melting, plutonism and extension (see text for details). Not to scale. Crust thickness is at least 50 km up to 20 Ma, at the onset of the opening of the Pannonia basin. Present crust thickness in the area is about 30 km.

melting of intermediate crust, which resulted in the genesis of the least evolved TMG magmas, which successively experienced AFC processes (Fig. 13e). Two-mica granite-like magmas were emplaced as a magmatic body, such as the Mt Bukulja pluton, and as veins and dykes intruding the main QMZD body, in the case of Mt Cer pluton. These magmatic intrusions were emplaced at about the 300–400 MPa level, producing strong contact metamorphic effects in the case of the Mt Bukulja pluton (Fig. 13e), whereas the present day outcrop level resulted from subsequent erosion processes (Fig. 13f).

Acknowledgements. We have dedicated this paper to late Prof. Vera Knežević-Đorđević, whose nearly four decades of research contributed greatly to the understanding of the origin of Serbian granites. We are grateful to N. Bonev, B. Bonin, two anonymous referees and editor D. Pyle for critical reviews and helpful comments, which greatly improved the manuscript. The authors thank Dejan Prelević and Diego Perugini for critical reading of early versions of the paper. We are very grateful to R. A. Creaser, Department of Earth and Atmospheric Sciences, University of Alberta, Canada, for Sr and Nd isotope analyses. This study was supported by a Scientific Exchange Programme between the Aristotle University of Thessaloniki and University of Belgrade and by the Project 146013 of the Serbian Ministry of Science and Technological Development (VC). Research was also financially supported by Italian MIUR and University of Perugia funds to GP. A grant to GC from European Commission TMR Programme – Geochemical facility was used for REE analyses in the Department of Earth Sciences, University of Bristol (UK).

References

AITCHESON, S. J. & FORREST, A. H. 1994. Quantification of crustal contamination in open magmatic systems. *Journal of Petrology* **35**, 461–88.

ALDERTON, D. H. M., PEARCE, J. A. & POTTS, P. J. 1980. Rare Earth Element mobility during granite alteration: evidence from Southwest England. *Earth and Planetary Science Letters* **49**, 149–65.

ALJINOVIĆ, B. 1987. On certain characteristics of the Mohorovicic discontinuity in the region of Yugoslavia. *Acta Geologica* **55**, 13–18.

ANDERSON, J. L. 1996. Status of thermobarometry in granitic batholiths. *Transactions of the Royal Society of Edinburgh: Earth Sciences* **87**, 125–38.

ANDERSON, J. L., BARTH, A. P., WOODEN, J. L. & MAZDAB, F. 2008. Thermometers and Thermobarometers in Granitic Systems. In *Minerals, Inclusions and Volcanic Processes* (eds K. D. Putirka & F. J. Tepley III), pp. 121–42. *Reviews in Mineralogy & Geochemistry* **69**.

https://doi.org/10.1017/S0016756810000476 Published online by Cambridge University Press

ANDERSON, J. L. & SMITH, D. R. 1995. The effects of temperature and f_{O_2} on the Al-in-hornblende barometer. *American Mineralogist* **80**, 549–59.

ANNEN, C., BLUNDY, J. D. & SPARKS, R. S. J. 2006. The Genesis of Intermediate and Silicic Magmas in Deep Crustal Hot Zones. *Journal of Petrology* **47**, 505–39.

BARBARIN, B. 2005. Mafic magmatic enclaves and mafic rocks associated with some granitoids of the central Sierra Nevada batholith, California: nature, origin, and relations with the hosts. *Lithos* **80**, 155–77.

BARBARIN, B. & DIDIER, J. 1991. Macroscopic features of mafic microgranular enclaves. In *Enclaves and granite petrology* (eds J. Didier & B. Barbarin), pp. 253–62. Developments in Petrology, no. 13. Amsterdam: Elsevier.

BATEMAN, R. 1995. The interplay between crystallization, replenishment and hybridization in large felsic magma chambers. *Earth Science Reviews* **39**, 91–106.

BLAKE, S. & FINK, J. H. 2000. On the deformation and freezing of enclaves during magma mixing. *Journal of Volcanology and Geothermal Research* **95**, 1–8.

BLUNDY, J. D. & SPARKS, R. S. J. 1992. Petrogenesis of mafic inclusions in granitoids of the Adamello Massif, Italy. *Journal of Petrology* **33**, 1039–1104.

BOTTINGA, Y. & WEILL, D. F. 1972. The viscosity of magmatic silicate liquids; a model calculation. *American Journal of Science* **272**, 438–75.

BRUNN, J. 1960. Mise en place et differenciation de l'association pluto-volcanique du cortege ophiolitique. *Revue de Geographie Physique et de Geologie Dynamique* **III**, 115–32.

CASTRO, A., MERENO-VENTAS, I. & DE LA ROSA, J. D. 1991. Multistage crystallization of tonalitic enclaves in granitoid rocks (Hercynian belt, Spain): implications for magma mixing. *Geologische Rundschau* **80**, 109–20.

CHEN, B., CHEN, Z. C. & JAHN, B. M. 2009. Origin of mafic enclaves from the Taihang Mesozoic orogen, north China craton. *Lithos* **110**, 343–58.

CHRISTOFIDES, G., PERUGINI, D., KORONEOS, A., SOLDATOS, T., POLI, G., ELEFTHERIADIS, G., DEL MORO, A. & NEIVA, A. M. 2007. Interplay between geochemistry and magma dynamics during magma interaction: an example from the Sithonia Plutonic Complex (NE Greece). *Lithos* **95**, 243–66.

CHRISTOFIDES, G., SOLDATOS, T., ELEFTHERIADIS, G. & KORONEOS, A. 1998. Chemical and isotopic evidence for source contamination and crustal assimilation in Hellenic Rhodope plutonic rocks. In *Tertiary Magmatism of the Rhodopian Region* (eds G. Christofides, P. Marchev & G. Serri), pp. 305–18. *Acta Vulcanologica* **10**, Special Volume. Pisa–Roma: Serra editor.

CLEMENS, J. D. 2006. Melting of the continental crust: fluid regimes, melting reactions and source-rock fertility. In *Evolution and Differentiation of the Continental Crust* (eds M. Brown & T. Rushmer), pp. 297–331. Cambridge: Cambridge University Press.

CLEMENS, J. D., YEARRON, L. M. & STEVENS, G. 2006. Barberton (South Africa) TTG magmas: Geochemical and experimental constraints on source-rock petrology, pressure of formation and tectonic setting. *Precambrian Research* **151**, 53–78.

COLLINS, W. J., RICHARDS, S. R., HEALY, B. E. & ELLISON, P. I. 2000. Origin of heterogeneous mafic enclaves by two-stage hybridisation in magma conduits (dykes) below and in granitic magma chambers. *Geological Society of America Special Papers* **350**, 27–45.

CVETKOVIĆ, V., KNEŽEVIĆ, V. & PÉCSKAY, Z. 2000. Tertiary igneous formations of the Dinarides, Vardar zone and adjacent regions: from recognition to petrogenetic implications. In *Geology and Metallogeny of the Dinarides and the Vardar zone* (ed. S. K. S. Janković), pp. 245–53. The Academy of Sciences and Arts of the Republic of Srpska, Bosnia and Herzegovina.

CVETKOVIĆ, V., KORONEOS, A., CHRISTOFIDES, G., POLI, G., KNEŽEVIĆ, V. & ERIĆ, V. 2002. Granitoids of Mt. Cer and Mt. Bukulja and their significance for geodynamics of the southern Pannonian realm. *Carpathian–Balkan Geological Association XVII, Bratislava Slovakia, Conference Abstract, CD-version*.

CVETKOVIĆ, V., POLI, G., CHRISTOFIDES, G., KORONEOS, A., PECSKAY, Z., RESIMIC-SARIC, K. & ERIC, V. 2007. The Miocene granitoid rocks of Mt. Bukulja (central Serbia): evidence for Pannonian extension-related granitoid magmatism in the northern Dinarides. *European Journal of Mineralogy* **19**, 513–32.

CVETKOVIĆ, V., PRELEVIĆ, D., DOWNES, H., JOVANOVIC, M., VASELLI, O. & PÉCSKAY, Z. 2004. Origin and geodynamic significance of Tertiary postcollisional basaltic magmatism in Serbia (central Balkan Peninsula). *Lithos* **73**, 161–86.

DE PAOLO, D. J. 1981. Trace element and isotopic effects of combined wallrock assimilation and fractional crystallization. *Earth and Planetary Science Letters* **53**, 189–202.

DIDIER, J. & BARBARIN, B. 1991. The different types of enclaves in granites – Nomenclature. In *Enclaves and Granite Petrology* (eds J. Didier & B. Barbarin), pp. 19–23. Developments in Petrology, no. 13. Amsterdam: Elsevier.

DONAIRE, T., PASCUAL, E., PIN, C. & DUTHOU, J.-L. 2005. Microgranular enclaves as evidence of rapid cooling in granitoid rocks: the case of the Los Pedroches granodiorite, Iberian Massif, Spain. *Contributions to Mineralogy and Petrology* **149**, 247–65.

ELBURG, M. A. 1996. Evidence of equilibration between microgranitoid enclaves and host granodiorite, Warburton Granodiorite, Lachlan Fold Belt, Australia. *Lithos* **38**, 1–22.

ELEFTHERIADIS, G., CHRISTOFIDES, G., MAVROUDCHIEV, B., NEDYALKOV, R., ANDREEV, A. & HRISTO, L. 1989. Tertiary volcanics from the East Rhodopes in Greece and Bulgaria. *Geologica Rhodopica* **1**, 202–17.

ELIAS, J. 1998. The thermal history of the Ötztal-Stubai complex (Tyrol, Austria/Italy) in the light of the lateral extrusion model. *Tübinger Geowissenschaftliche Arbeiten Reihe A* **36**, 172 pp.

ENGLAND, P. & HOUSEMAN, G. 1985. Role of lithospheric strength heterogeneities in the tectonics of Tibet and neighbouring regions. *Nature* **315**, 297–301.

FILIPOVIĆ, I., SIKOŠEK, B. & JOVANOVIĆ, D. 1993. Paleozoic Complexes of Northwestern Serbia Formation Conodonts. *Annales Géologiques de la Péninsule Balkanique, Belgrade* **57**, 71–83.

FODOR, L., GERDES, A., DUNKL, I., KOROKNAI, B., PÉCSKAY, Z., TRAJANOVA, M., HORVÁTH, P., VRABEC, M., JELEN, B., BALOGH, K. & FRISCH, W. 2008. Miocene emplacement and rapid cooling of the Pohorje pluton at the Alpine–Pannonian–Dinaridic junction, Slovenia. *Swiss Journal of Geosciences* **101**, 255–71.

FOURCADE, S. & ALLÈGRE, C. J. 1981. Trace element behaviour in granite genesis, a case study of the calc-alkaline plutonic association from the Querigut

Complex Pyrenees, France. *Contributions to Mineralogy and Petrology* **76**, 177–95.

GAGNEVIN, D., WAIGHT, T. E., DALY, J. S., POLI, G. & CONTICELLI, S. 2007. Insights into magmatic evolution and recharge history in Capraia Volcano (Italy) from chemical and isotopic zoning in plagioclase phenocrysts. *Journal of Volcanology and Geothermal Research* **168**, 28–54.

HAMMARSTROM, J. M. & ZEN, E-AN. 1986. Aluminum in hornblende; an empirical igneous geobarometer. *American Mineralogist* **71**, 1297–1313.

HASKIN, L. A., FREY, F. A., SCHMITT, R. A. & SMITH, R. H. 1966. Meteoritic, solar and terrestrial rare-earth distributions. In *Physics and Chemistry of the Earth* (eds L. H. Ahrens, F. Press, S. K. Runcorn & H. C. Urey), pp. 167–321. New York: Pergamon Press.

HIBBARD, M. 1995. *Petrography to Petrogenesis*. Englewood Cliffs, New Jersey: Prentice Hall, 587 pp.

HOLLAND, T. & BLUNDY, J. 1994. Non-ideal interactions in calcic amphiboles and their bearing on amphibole–plagioclase thermometry. *Contributions to Mineralogy and Petrology* **116**, 433–47.

ILIĆ, A. & NEUBAUER, F. 2005. Tertiary to recent oblique convergence and wrenching of the Central Dinarides: Constraints from a palaeostress study. *Tectonophysics* **410**, 465–84.

JANOUSEK, V., BRAITHWAITE, C. J. R., BOWES, D. R. & GERDES, A. 2004. Magma-mixing in the genesis of Hercynian calc-alkaline granitoids: an integrated petrographic and geochemical study of the Sázava intrusion, Central Bohemian Pluton, Czech Republic. *Lithos* **78**, 67–99.

KARAMATA, S. 2006. The geological development of the Balkan Peninsula related to the approach, collision and compression of Gondwanan and Eurasian units. In *Tectonic Development of the Eastern Mediterranean Region* (eds A. H. F. Robertson & D. Mountrakis), pp. 155–78. Geological Society of London, Special Publication no. 260.

KARAMATA, S., DELALOYE, M., LOVRIĆ, A. & KNEŽEVIĆ, V. 1992*a*. Two genetic groups of Tertiary granitic rocks of central and western Serbia. *Annales Géologiques de la Péninsule Balkanique* **56**, 263–83.

KARAMATA, S., STEIGER, R., ĐORĐEVIĆ, P. & KNEŽEVIĆ, V. 1990. New data on the origin of granitic rocks from western Serbia. *Bulletin de l'Académie Serbe des Sciences et des Arts, Classe des Sciences mathématiques et naturelles, Science naturelles* **CII**, 1–9.

KARAMATA, S., STOJANOV, R., SERAFIMOVSKI, T., BOEV, B. & ALEKSANDROV, M. 1992*b*. Tertiary magmatism of the Vardar Zone of the Dinarides and Serbo-Macedonian Massif. *Geologia Macedonica* **6**, 127–86.

KARAMATA, S., VASKOVIĆ, N., CVETKOVIĆ, V. & KNEŽEVIĆ-ĐORĐEVIĆ, V. 1994. Upper Cretaceous and Tertiary igneous rocks of the central and eastern Serbia and their metallogeny. *Annales Géologiques de la Péninsule Balkanique* **58**, 159–75.

KARSLI, O., CHEN, B., AYDIN, F. & SEN, C. 2007. Geochemical and Sr–Nd–Pb isotopic compositions of the Eocene Dölek and Sariçiçek Plutons, Eastern Turkey: implications for magma interaction in the genesis of high-K calc-alkaline granitoids in a post-collision extensional setting. *Lithos* **98**, 67–96.

KELEMEN, P. B., HANGHØJ, K., GREENE, A. R., HEINRICH, D. H. & KARL, K. T. 2007. One View of the Geochemistry of Subduction-Related Magmatic Arcs, with an Emphasis on Primitive Andesite and Lower Crust. In *Treatise on Geochemistry* (ed. R. L. Rudnick), pp. 1–70. Oxford: Pergamon.

KIRSCHBAUM, A., MARTÍNEZ, E., PETTINARI, G. & HERRERO, S. 2005. Weathering profiles in granites, Sierra Norte (Córdoba, Argentina). *Journal of South American Earth Sciences* **19**, 479–93.

KNEŽEVIĆ, V. 1962. The origin and petrochemical character of igneous and contact metamorphic rocks of mountain Cer. *Transactions of the Mining and Geological Faculty Beograd for 1959/1960* **7**, 190–201.

KNEŽEVIĆ, V., CVETKOVIĆ, V. & RESIMIĆ, K. 1997. Granodiorites of Stražanica on the western slopes of Cer Mt. (western Serbia). *Annales Géologiques de la Péninsule Balkanique* **61**, 311–24.

KNEŽEVIĆ, V., KARAMATA, S. & CVETKOVIĆ, V. 1994. Tertiary granitic rocks along the southern margin of the Pannonian basin. *Acta Mineralogica-Petrographica (Szeged)* **XXXV**, 71–80.

KRETZ, R. 1983. Symbols for rock-forming minerals. *American Mineralogist* **68**, 277–9.

LABAŠ, V. 1975. Građa Motajice prema rezultatima gravimetrijskih ispitivanja. *Panel diskusija o pregibnoj zoni Unutrašnjih Dinarida, Zagreb Serija B* Knj. **6**, 45–51.

LANGMUIR, C. H., VOCKE, R. D. JR, HANSON, G. N. & HART, S. R. 1978. A general mixing equation with applications to Icelandic basalts. *Earth and Planetary Science Letters* **37**, 380–92.

LAUBSCHER, H. 1983. The Late Alpine (Periadriatic) intrusions and the Insubric line. *Memorie della Società Geologica Italiana* **26**, 21–30.

LESHER, C. E. 1990. Decoupling of chemical and isotopic exchange during magma mixing. *Nature* **344**, 235–7.

LIANG, Y., RICHTER, F. M. & WATSON, E. B. 1996. Diffusion in silicate melts: II. Multicomponent diffusion in CaO–Al_2O_3–SiO_2 at 1500°C and 1 GPa. *Geochimica et Cosmochimica Acta* **60**, 5021–35.

LIÉGEOIS, J.-P., NAVEZ, J., HERTOGEN, J. & BLACK, R. 1998. Contrasting origin of post-collisional high-K calc-alkaline and shoshonitic versus alkaline and peralkaline granitoids. The use of sliding normalization. *Lithos* **45**, 1–28.

LONG, L. E., CASTELLANA, C. H. & SIAL, A. N. 2005. Age, Origin and Cooling History of the Coronel João Sá Pluton, Bahia, Brazil. *Journal of Petrology* **46**, 255–73.

MAKRIDAKIS, S., WHEELWRIGHT, S. & HYNDMAN, R. 1998. *Forecasting: Methods and Applications*. New York: Wiley, 640 pp.

MAROVIĆ, M., KRSTIĆ, N., STANIĆ, S., CVETKOVIĆ, V. & PETROVIĆ, M. 1999. The evolution of Neogene sedimentation provinces of Central Balkan Peninsula. *Bulletin of Geoinstitute Belgrade* **36**, 25–94.

MAROVIĆ, M., MIHAILOVIĆ, D., ĐOKOVIĆ, I., GERZINA, N. & TOLJIĆ, M. 2001. Wrench tectonics of the Paleogene–Lower Miocene basins of Serbia between the central part of the Vardar Zone and the Moesian Plate. *PANCARDI 2001, Sopron Conference Abstract*, p. 28.

MAVROUDCHIEV, B., NEDYALKOV, R., ELEFTHERIADIS, G., SOLDATOS, T. & CHRISTOFIDES, G. 1993. Tertiary plutonic rocks from east Rhodope in Bulgaria and Greece. *Bulletin of the Geological Society of Greece* **XXVIII**, 643–60.

MCDONOUGH, W. F., SUN, S. S., RINGWOOD, A. E., JAGOUTZ, E. & HOFMANN, A. W. 1992. Potassium, rubidium, and cesium in the Earth and Moon and the

evolution of the mantle of the Earth. *Geochimica et Cosmochimica Acta* **56**, 1001–12.

McDougall, I. & Harrison, T. M. 1999. *Geochronology and thermochronology by the $^{40}Ar/^{39}Ar$ method*. New York: Oxford University Press, 269 pp.

Nakamura, E. & Kushiro, I. 1998. Trace element diffusion in jadeite and diopside melts at high pressures and its geochemical implication. *Geochimica et Cosmochimica Acta* **62**, 3151–60.

Nitoi, E., Munteanu, M., Marincea, S. & Paraschivoiu, V. 2002. Magma-enclave interactions in the East Carpathian Subvolcanic Zone, Romania: petrogenetic implications. *Journal of Volcanology and Geothermal Research* **118**, 229–59.

Pamić, J. 1977. Alpski magmatsko-metamorfni procesi kao indikatori geološke evolucije terena sjeverne Bosne. *Geološki glasnik (Bulletin géologique)* **22**, 257–92 (in Croatian with English summary).

Pamić, J. 1985/1986. Kredno-tercijarne granitne i metamorfne stijene u dodirnom području sjevernih Dinarida i Panonskog strukturnog kompleksa *Geologija – Razprave in poročila Ljubljana* **28/29**, 219–37 (in Croatian with English abstract).

Pamić, J., Balen, D. & Herak, M. 2002,. Origin and geodynamic evolution of Late Paleogene magmatic associations along the Periadriatic-Sava-Vardar magmatic belt. *Geodinamica Acta* **15**, 209–31.

Peccerillo, A. & Taylor, S. R. 1976. Geochemistry of Eocene calc-alkaline volcanic rocks from the Kastamonu area, northern Turkey. *Contribution to Mineralogy and Petrology* **58**, 63–81.

Pécskay, Z., Knežević, V., Cvetković, V. & Resimić-Šarić, K. 2001. Time and space distribution of Tertiary granitoid rocks of Serbia: geodynamic implications. *PANCARDI 2001 Sopron, Conference abstract, DP-14*.

Pe-Piper, G. 2007. Relationship of amphibole composition to host-rock geochemistry: the A-type gabbro-granite Wentworth pluton, Cobequid shear zone, eastern Canada. *European Journal of Mineralogy* **19**, 29–38.

Perugini, D. & Poli, G. 2005. Viscous fingering during replenishment of felsic magma chambers by continuous inputs of mafic magmas: Field evidence and fluid-mechanics experiments. *Geology* **33**, 5–8.

Perugini, D., Poli, G., Christofides, G. & Eleftheriadis, G. 2003. Magma mixing in the Sithonia Plutonic Complex, Greece: evidence from mafic microgranular enclaves. *Mineralogy and Petrology* **78**, 173–200.

Pitcher, W. S. 1997. *The Nature and Origin of Granite*. London: Chapman & Hall, 387 pp.

Poli, G. & Tommasini, S. 1991. Model for the origin and significance of microgranular enclaves in calc-alkaline granitoids. *Journal of Petrology* **32**, 657–66.

Poli, G. & Tommasini, S. 1999. Insights on acid-basic magma interaction from the Sardinia–Corsica batholith: the case study of Sarrabus, southeastern Sardinia, Italy. *Lithos* **46**, 553–71.

Poli, G., Tommasini, S. & Halliday, A. N. 1996. Trace elements and isotopic exchange during acid-basic magma interaction processes. *Transactions of the Royal Society of Edinburgh: Earth Sciences* **87**, 225–32.

Prelević, D., Foley, S. F. & Cvetković, V. 2007. A review of petrogenesis of Mediterranean Tertiary lamproites: a perspective from the Serbian ultrapotassic province. In *Cenozoic Volcanism in the Mediterranean Area* (eds L. Beccaluva, G. Bianchini & M. Wilson), pp. 113–29. *GSA Special Papers* **418**.

Prelević, D., Foley, S. F., Cvetković, V. & Romer, R. L. 2004. Origin of minette by mixing of lamproite and dacite magmas in Veliki Majdan, Serbia. *Journal of Petrology* **45**, 759–92.

Prelević, D., Foley, S. F., Romer, R. L., Cvetković, V. & Downes, H. 2005. Tertiary ultrapotassic volcanism in Serbia: constraints on petrogenesis and mantle source characteristics. *Journal of Petrology* **46**, 1443–87.

Qin, J., Lai, S., Grapes, R., Diwu, C., Ju, Y. & Li, Y. 2009. Geochemical evidence for origin of magma mixing for the Triassic monzonitic granite and its enclaves at Mishuling in the Qinling orogen (central China). *Lithos* **112**, 259–76.

Rapp, R. P. & Watson, E. B. 1995. Dehydration melting of metabasalt at 8–32 kbar: implications for continental growth and crust-mantle recycling. *Journal of Petrology* **36**, 891–931.

Ratschbacher, L., Frisch, W., Neubauer, F., Schmid, S. M. & Neugebauer, J. 1989. Extension in compressional orogenic belts: the eastern Alps. *Geology* **17**, 404–7.

Robertson, A., Karamata, S. & Sarić, K. 2009. Overview of ophiolites and related units in the Late Palaeozoic–Early Cenozoic magmatic and tectonic development of Tethys in the northern part of the Balkan region. *Lithos* **108**, 1–36.

Rollinson, H. 1993. *Using geochemical data: Evaluation, presentation, interpretation*. Longman Scientific & Technical, 352 pp.

Rosenberg, C. L. 2004. Shear zones and magma ascent: A model based on a review of the Tertiary magmatism in the Alps. *Tectonics* **23**, 1–21.

Schmid, S., Bernoulli, D., Fügenschuh, B., Matenco, L., Schefer, S., Schuster, R., Tischler, M. & Ustaszewski, K. 2008. The Alpine–Carpathian–Dinaridic orogenic system: correlation and evolution of tectonic units. *Swiss Journal of Geosciences* **101**, 139–83.

Schmidt, M. W. 1992. Amphibole composition in tonalite as a function of pressure: an experimental calibration of the Al-in-hornblende barometer. *Contributions to Mineralogy and Petrology* **110**, 304–10.

Sen, C. & Dunn, T. 1994. Dehydration melting of a basaltic composition amphibolite at 1.5 and 2.0 GPa: implications for the origin of adakites. *Contributions to Mineralogy and Petrology* **117**, 394–409.

Shaw, H. R. 1972. Viscosities of magmatic silicate liquids; an empirical method of prediction. *American Journal of Science* **272**, 870–93.

Snyder, D. & Tait, S. 1998. The imprint of basalt on the geochemistry of silicic magmas. *Earth and Planetary Science Letters* **160**, 433–45.

Sparks, R. S. J. & Marshall, L. A. 1986. Thermal and mechanical constraints on mixing between mafic and silicic magmas. *Journal of Volcanology and Geothermal Research* **29**, 99–124.

Steiger, R. H., Knežević, V. & Karamata, S. 1989. Origin of some granitic rocks from the southern margin of the Panonian basin in Western Serbia, Yugoslavia. *EUG V Strasbourg France Conference Abstract*, 52–3.

Stein, E. & Dietl, C. 2001. Hornblende thermobarometry of granitoids from the Central Odenwald (Germany) and their implications for the geotectonic development of the Odenwald. *Mineralogy and Petrology* **72**, 185–207.

Streckeisen, A. & Le Maitre, R. W. 1979. A chemical approximation to the modal QAPF classification of

igneous rocks. *Neues Jahrbuch für Mineralogie Abhandlungen* **136**, 169–206.

VERNON, R. H. 1984. Microgranitoid enclaves in granites – globules of hybrid magma quenched in a plutonic environment. *Nature* **309**, 438–9.

VON BLANCKENBURG, F., FRÜH-GREEN, G., DIETHELM, K. & STILLE, P. 1992. Nd-, Sr-, O-isotopic and chemical evidence for a two-stage contamination history of mantle magma in the Central-Alpine Bergell intrusion. *Contributions to Mineralogy and Petrology* **110**, 33–45.

VON BLANCKENBURG, F. & DAVIES, J. H. 1995. Slab breakoff: A model for syncollisional magmatism and tectonics in the Alps. *Tectonics* **14**, 120–31.

VON BLANCKENBURG, F., KAGAM, I. H., DEUTSCH, A., OBERLI, F., MEIER, M., WIEDENBECK, M., BARTH, S. & FISCHER, H. 1998. The origin of Alpine plutons along the Periadriatic Lineament. *Schweizerische Mineralogische und Petrographische Mitteilungen* **78**, 55–66.

VYHNAL, C., MCSWEEN, H. JR & SPEER, J. 1991. Hornblende chemistry in southern Appalachian granitoids: implications for aluminum hornblende thermobarometry and magmatic epidote stability. *American Mineralogist* **76**, 176–88.

WAIGHT, T. E., MAAS, R. & NICHOLLS, I. A. 2001. Geochemical investigations of microgranitoid enclaves in the S-type Cowra Granodiorite, Lachlan Fold Belt, SE Australia. *Lithos* **56**, 165–86.

WEI, L., CONGQIANG, L. & MASUDA, A. 1997. Complex trace-element effects of mixing-fractional crystallization composite processes: applications to the Alaer granite pluton, Altay Mountains, Xinjiang, northwestern China. *Chemical Geology* **135**, 103–24.

WOOD, D. A., JORON, J. L., TREUIL, M., NORRY, M. & TARNEY, J. 1979. Elemental and Sr isotope variations in basic lavas from Iceland and the surrounding ocean floor. *Contributions to Mineralogy and Petrology* **70**, 319–39.

WRIGHT, T. L. & DOHERTY, P. C. 1970. A linear programming and least squares computer method for solving petrologic mixing problems. *Geological Society of America Bulletin* **81**, 1995–2008.

ZEN, E.-A. & HAMMARSTROM, J. M. 1984. Magmatic epidote and its petrologic significance. *Geology* **12**, 515–18.

ZHANG, S. H., ZHAO, Y. & SONG, B. 2006. Hornblende thermobarometry of the Carboniferous granitoids from the Inner Mongolia Paleo-uplift: implications for the tectonic evolution of the northern margin of North China block. *Mineralogy and Petrology* **87**, 123–41.